Compact stars in the QCD phase diagram VI

Dubna, 29. 9. 2017

Correlations and bound states in nuclear matter

Gerd Röpke, Rostock

Outline

- Clustering in low-density nuclei and nuclear matter. Nonequilibrium and equilibrium, Zubarev approach
- Equation of state: quantum statistical approach to nuclear systems at finite temperatures and subsaturation densities,
  bound states, spectral function, quasiparticle concept
- Light quasiparticles: self-energy and Pauli blocking, Continuum correlations, cluster virial expansion, correlated matter
- Dynamical response
- Heavy elements, thermodynamic instability, pasta structures
- Neutron star crust
- HIC: chemical constants, symmetry energy
- Transport codes, Mott effect and in-medium cross sections, relevance of the equilibrium EoS. Light cluster production at NICA

Symmetric nuclear matter: Phase diagram

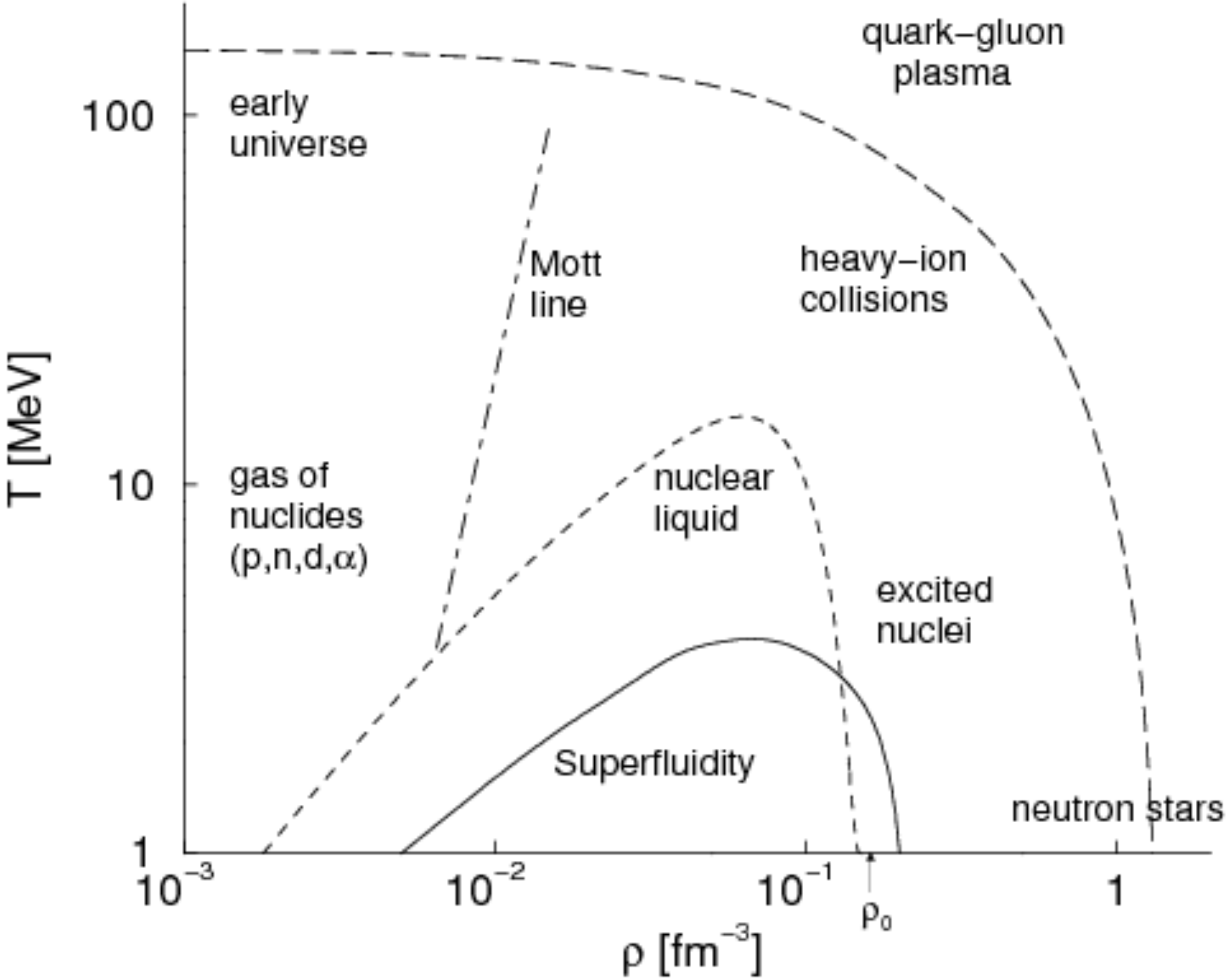

Light cluster production at NICA★

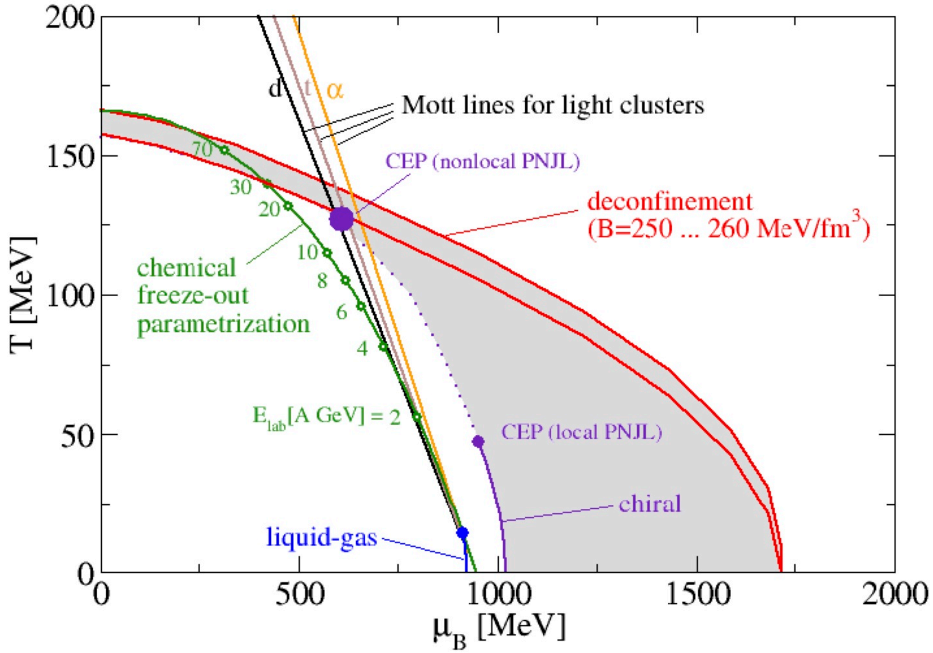

Fig. 1. Phase diagram of dense nuclear matter in the plane of temperature T and baryochemical potential μ_B. The diagram includes Mott lines for the dissociation of light nuclear clusters, extrapolated also to the deconfinement region. For details, see text.

N.-U. Bastian, P. Batyuk, D. Blaschke, P. Danielewicz, Yu.B. Ivanov, Iu. Karpenko, G. Ropke, O. Rogachevsky, and H.H. Wolter, Eur. Phys. J. A (2016) 52: 244

Equilibrium and non-equilibrium

Statistical operator $\varrho(t)$

Extended von Neumann equation

$$\frac{\partial}{\partial t}\varrho_\varepsilon(t) + \frac{i}{\hbar}\left[H, \varrho_\varepsilon(t)\right] = -\varepsilon\left(\varrho_\varepsilon(t) - \varrho_{\rm rel}(t)\right)$$

The relevant statistical operator $\varrho_{\rm rel}(t)$ is obtained from the maximum of entropy reproducing the local, time dependent composition with parameter values $T(\mathbf{r},t), \mu_n(\mathbf{r},t), \mu_p(\mathbf{r},t)$, but contains in addition the cluster distribution functions $f_{A\nu}^{\rm Wigner}(\mathbf{p},\mathbf{r},t)$ as relevant observables.[106,107]

$$\varrho(t) = \lim_{\varepsilon\to 0}\varrho_\varepsilon(t)$$

D.N. Zubarev, V.G. Morozov, and G. Ropke, Statistical Mechanics of Nonequilibrium Processes (1996)
D.N. Zubarev, V.G. Morozov, I.P. Omelyan, and M.V. Tokarchuk, Theoret. Math. Phys. **96**, 997 (1993)
G. Ropke and H. Schulz, Nucl. Phys. A **477**, 472 (1988)

Many-particle theory

- equilibrium correlation functions

  e.g. equation of state $n(\beta,\mu) = \frac{1}{\Omega_0} \sum_1 \langle a_1^\dagger a_1 \rangle$

  density matrix $\langle a_1^\dagger a_{1'} \rangle = \int \frac{\mathrm{d}\omega}{2\pi}\, \mathrm{e}^{-i\omega t} f_1(\omega) A(1,1',\omega)$

- Spectral function

$$A(1,1',\omega) = \mathrm{Im}\left[G(1,1',\omega+i\eta) - G(1,1',\omega-i\eta)\right]$$

- Matsubara Green function

$$G(1,1',iz_\nu), \qquad z_\nu = \frac{\pi\nu}{\beta} + \mu, \quad \nu = \pm1, \pm3, \cdots$$

$$1 \equiv \{\mathbf{p}_1, \sigma_1, c_1\}, \quad f_1(\omega) = \frac{1}{\mathrm{e}^{\beta(\omega-\mu)}+1}, \quad \Omega_0 - \text{volume}$$

Many-particle theory

- Dyson equation and self energy (homogeneous system)

$$G(1, iz_\nu) = \frac{1}{iz_\nu - E(1) - \Sigma(1, iz_\nu)}$$

- Evaluation of $\Sigma(1, iz_\nu)$:
  perturbation expansion, diagram representation

$$A(1,\omega) = \frac{2\mathrm{Im}\,\Sigma(1, \omega + i0)}{[\omega - E(1) - \mathrm{Re}\,\Sigma(1,\omega)]^2 + [\mathrm{Im}\,\Sigma(1, \omega + i0)]^2}$$

approximation for self energy $\longrightarrow$ approximation for equilibrium correlation functions

alternatively: simulations, path integral methods

Different approximations

- Expansion for small Im $\Sigma(1, \omega + i\eta)$

$$A(1,\omega) \approx \frac{2\pi\delta(\omega - E^{\text{quasi}}(1))}{1 - \frac{\mathrm{d}}{\mathrm{d}z}\mathrm{Re}\ \Sigma(1,z)|_{z=E^{\text{quasi}}-\mu_1}} \\ -2\mathrm{Im}\ \Sigma(1,\omega+i\eta)\frac{\mathrm{d}}{\mathrm{d}\omega}\frac{P}{\omega+\mu_1-E^{\text{quasi}}(1)}$$

quasiparticle energy $E^{\text{quasi}}(1) = E(1) + \mathrm{Re}\ \Sigma(1,\omega)|_{\omega=E^{\text{quasi}}}$

- chemical picture: bound states $\hat{=}$ new species

summation of ladder diagrams, Bethe-Salpeter equation

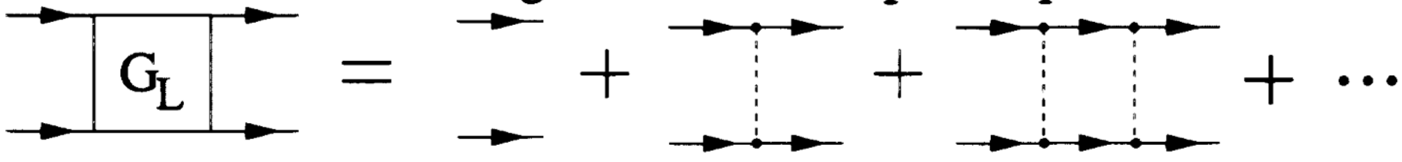

Different approximations

Ideal Fermi gas:

protons, neutrons,
(electrons, neutrinos,…)

bound state formation

Nuclear statistical equilibrium:

ideal mixture of all bound states
(clusters:) chemical equilibrium

medium effects

Quasiparticle quantum liquid:

mean-field approximation
Skyrme, Gogny, RMF

Quasiparticle picture: RMF and DBHF

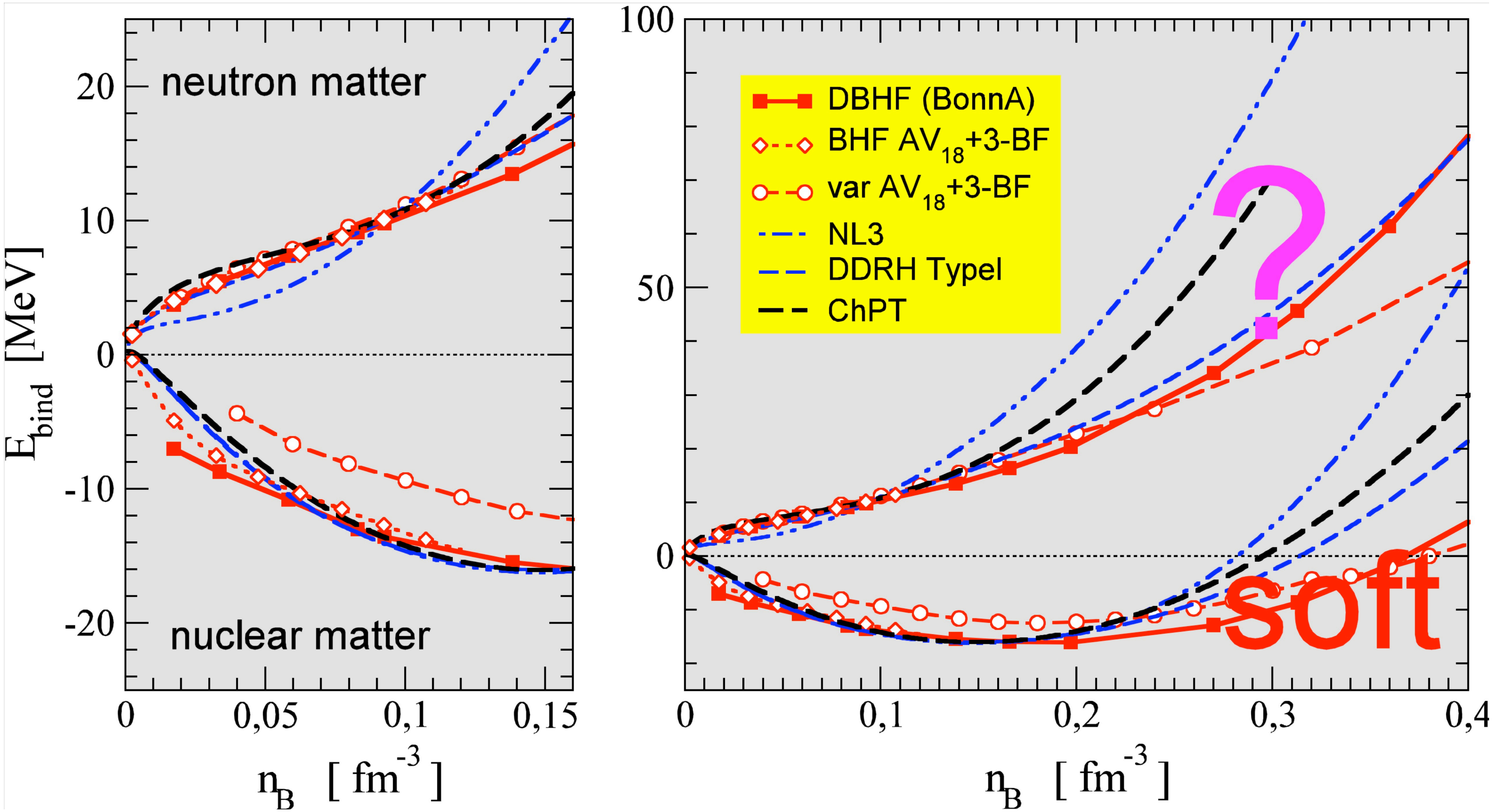

But: cluster formation

Incorrect low-density limit

C. Fuchs, H.H. Wolter, Eur. Phys. J. A **30**, 5 (2006)

Quasiparticle approximation for nuclear matter

Equation of state for symmetric matter

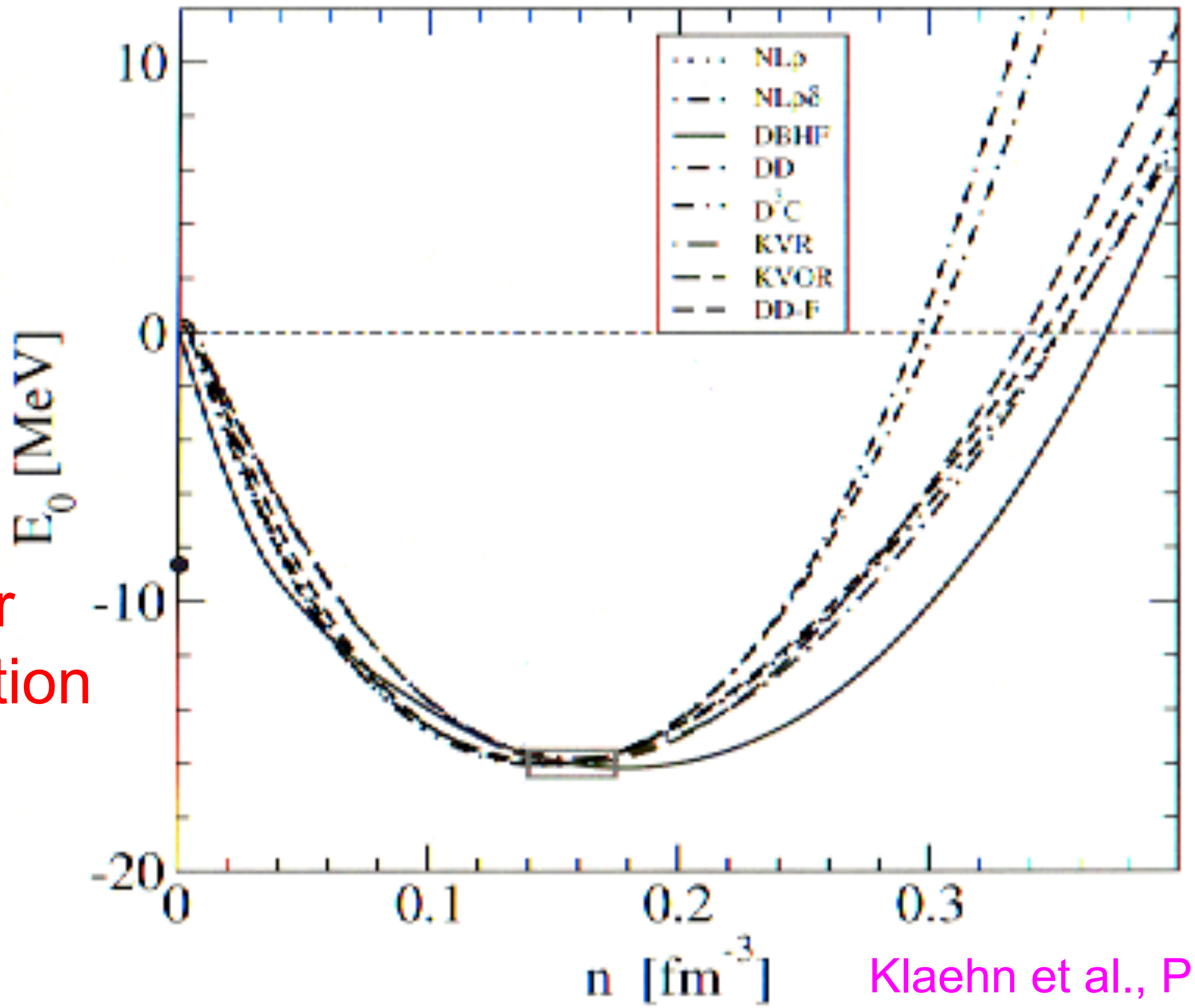

But: cluster formation

Incorrect low-density limit

Klaehn et al., PRC 2006

Nuclear statistical equilibrium (NSE)

Chemical picture:

Ideal mixture of reacting components

Mass action law

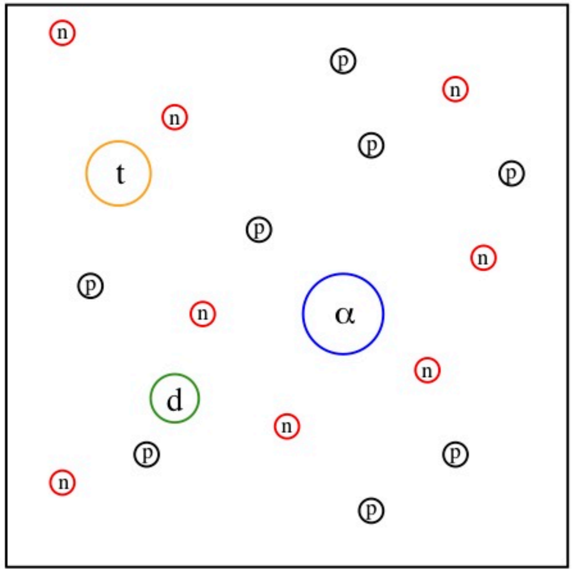

from S. Typel

Ideal mixture of reacting nuclides

$$
\begin{aligned}
n_p(T, \mu_p, \mu_n) &= \frac{1}{V} \sum_{A,\nu,K} Z_A f_A\{E_{A,\nu K} - Z_A \mu_p - (A - Z_A)\mu_n\} \\
n_n(T, \mu_p, \mu_n) &= \frac{1}{V} \sum_{A,\nu,K} (A - Z_A) f_A\{E_{A,\nu K} - Z_A \mu_p - (A - Z_A)\mu_n\}
\end{aligned}
$$

mass number A,
charge Z_A,
energy $E_{A,\nu,K}$,
ν internal quantum number,
$\tilde{K}$ center of mass momentum

$$
f_{A(z)} = \frac{1}{\exp(z/T) - (-1)^A}
$$

Chemical equilibrium, mass action law,
Nuclear Statistical Equilibrium (NSE)

Nuclear statistical equilibrium (NSE)

Chemical picture:

Ideal mixture of reacting components

Mass action law

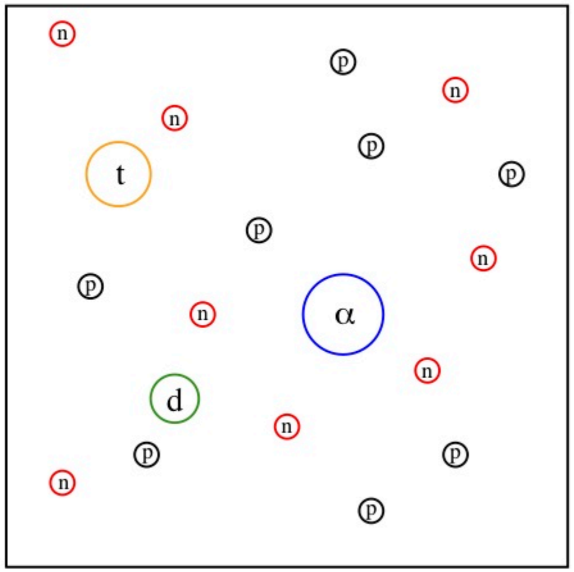

Interaction between the components
internal structure: Pauli principle

Physical picture:

"elementary" constituents
and their interaction

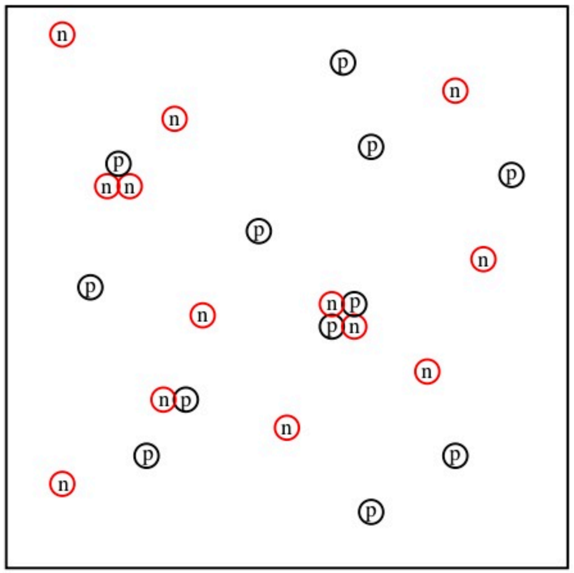

Quantum statistical (QS) approach,
quasiparticle concept, virial expansion

Different approximations

medium effects

Ideal Fermi gas:
protons, neutrons,
(electrons, neutrinos,…)

Quasiparticle quantum liquid:
mean-field approximation
Skyrme, Gogny, RMF

bound state formation

Nuclear statistical equilibrium:
ideal mixture of all bound states
(clusters:) chemical equilibrium

Chemical equilibrium with quasiparticle clusters:
self-energy and Pauli blocking

Effective wave equation for the deuteron in matter

In-medium two-particle wave equation in mean-field approximation

$$\left(\frac{p_1^2}{2m_1}+\Delta_1+\frac{p_2^2}{2m_2}+\Delta_2\right)\Psi_{d,P}(p_1,p_2)+\sum_{p_1',p_2'}(1-f_{p_1}-f_{p_2})V(p_1,p_2;p_1',p_2')\Psi_{d,P}(p_1',p_2')$$

$$=E_{d,P}\Psi_{d,P}(p_1,p_2)$$

Add self-energy

Pauli-blocking

Thouless criterion

$$E_d(T,\mu)=2\mu$$

Fermi distribution function

$$f_p=\left[e^{(p^2/2m-\mu)/k_BT}+1\right]^{-1}$$

BEC-BCS crossover:
Alm et al.,1993

Pauli blocking – phase space occupation

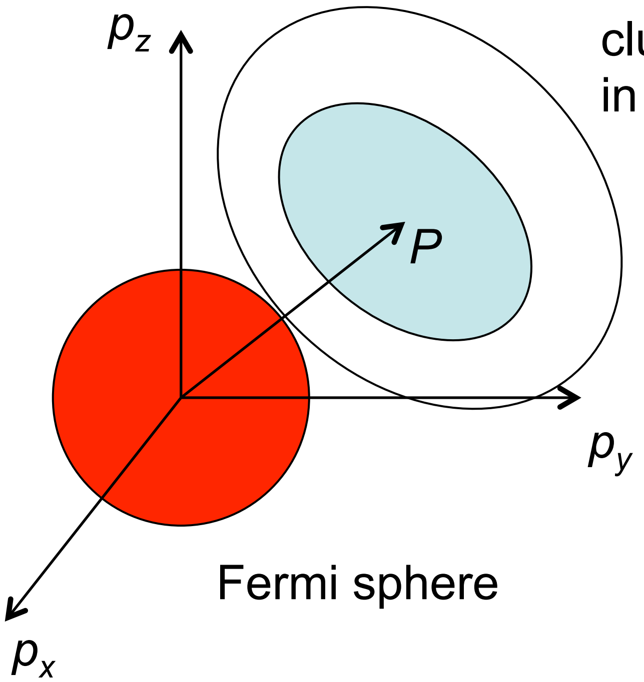

cluster wave function (deuteron, alpha,…)
in momentum space

P - center of mass momentum

The Fermi sphere is forbidden,
deformation of the cluster wave function
in dependence on the c.o.m. momentum P

momentum space

The deformation is maximal at $P = 0$.
It leads to the weakening of the interaction
(disintegration of the bound state).

Shift of the deuteron binding energy

Dependence on nucleon density, various temperatures,
zero center of mass momentum

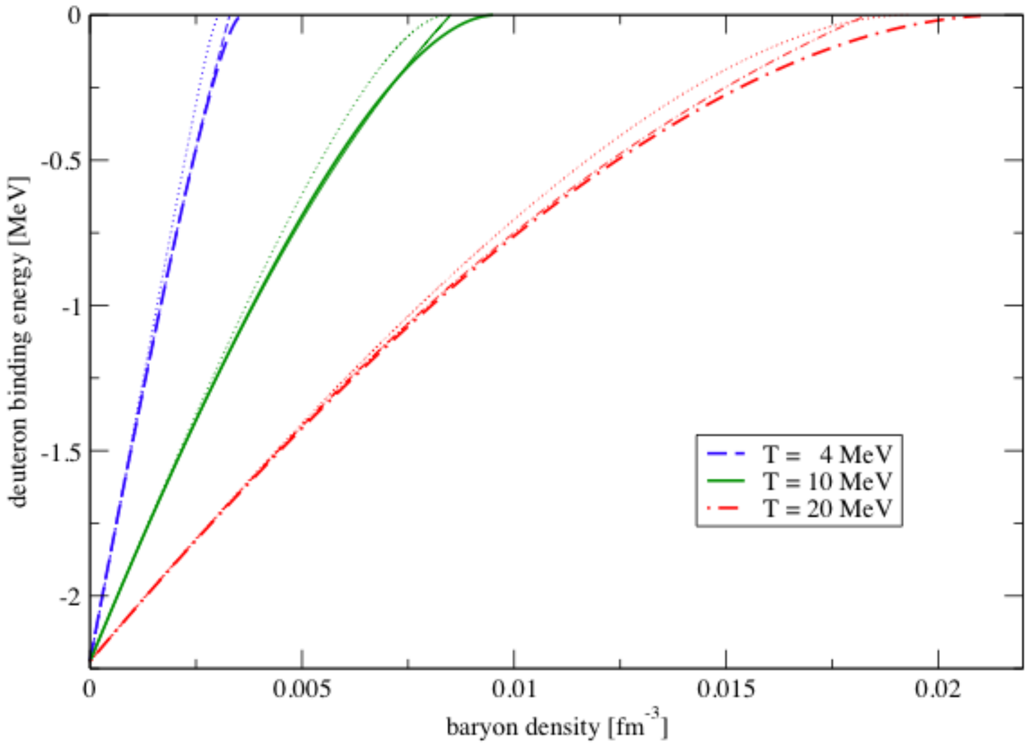

thin lines:

fit formula

G.R., NP A **867**, 66 (2011)

Few-particle Schrödinger equation in a dense medium

4-particle Schrödinger equation with medium effects

$$\left(\left[E^{HF}(p_1)+E^{HF}(p_2)+E^{HF}(p_3)+E^{HF}(p_4)\right]\right)\Psi_{n,P}(p_1,p_2,p_3,p_4)$$

$$+\sum_{p_1',p_2'}(1-f_{p_1}-f_{p_2})V(p_1,p_2;p_1',p_2')\Psi_{n,P}(p_1',p_2',p_3,p_4)$$

$$+\{permutations\}$$

$$=E_{n,P}\Psi_{n,P}(p_1,p_2,p_3,p_4)$$

Composition of dense nuclear matter

$$n_p(T,\mu_p,\mu_n) = \frac{1}{V}\sum_{A,\nu,K} Z_A f_A\{E_{A,\nu K} - Z_A\mu_p - (A-Z_A)\mu_n\}$$

$$n_n(T,\mu_p,\mu_n) = \frac{1}{V}\sum_{A,\nu,K} (A-Z_A) f_A\{E_{A,\nu K} - Z_A\mu_p - (A-Z_A)\mu_n\}$$

mass number A
charge Z_A
energy $E_{A,\nu,K}$
ν: internal quantum number

$$f_{A(z)} = \frac{1}{\exp(z/T) - (-1)^A}$$

- Medium effects: correct behavior near saturation
  self-energy and Pauli blocking shifts of binding energies,
  Coulomb corrections due to screening (Wigner-Seitz,Debye)

- Inclusion of excited states and continuum correlations,
  correct virial expansions

- Bose-Einstein condensation, phase instabilities

Different approximations

Ideal Fermi gas:
protons, neutrons,
(electrons, neutrinos,…)

medium effects

Quasiparticle quantum liquid:
mean-field approximation
Skyrme, Gogny, RMF

bound state formation

Nuclear statistical equilibrium:
ideal mixture of all bound states
(clusters:) chemical equilibrium

Chemical equilibrium
with quasiparticle clusters:
self-energy and Pauli blocking

continuum contribution

Second virial coefficient:
account of continuum contribution,
scattering phase shifts, Beth-Uhl.E.

Generalized Beth-Uhlenbeck
formula:
medium modified binding energies,
medium modified scattering phase shifts

Deuteron-like scattering phase shifts

Virial coeff. $\propto e^{-E_d^0/T} - 1 + \frac{1}{\pi T}\int_0^\infty dE\; e^{-E/T}\left\{\delta_c(E) - \frac{1}{2}\sin[2\delta_c(E)]\right\}$

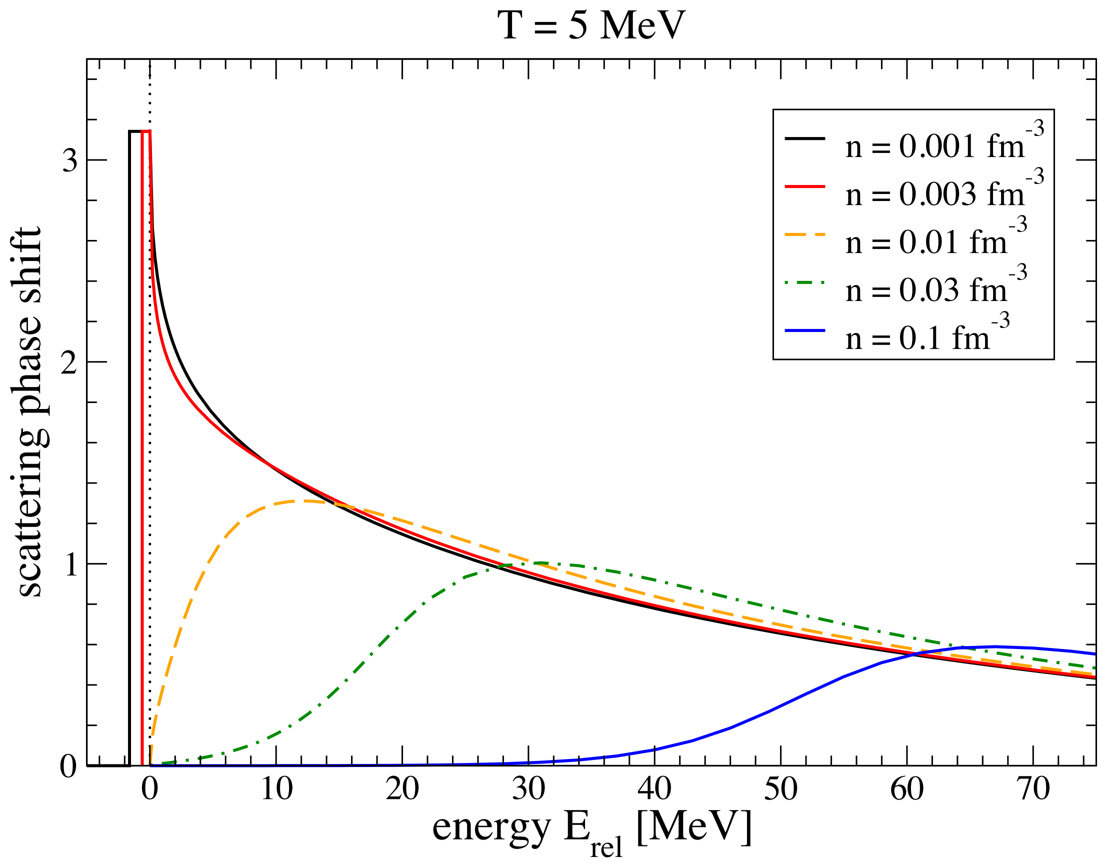

deuteron bound state -2.2 MeV

G. Roepke, J. Phys.: Conf. Series 569, 012031 (2014).

Different approximations

medium effects

Ideal Fermi gas:
protons, neutrons,
(electrons, neutrinos,…)

Quasiparticle quantum liquid:
mean-field approximation
Skyrme, Gogny, RMF

bound state formation

Nuclear statistical equilibrium:
ideal mixture of all bound states
(clusters:) chemical equilibrium

Chemical equilibrium
with quasiparticle clusters:
self-energy and Pauli blocking

continuum contribution

Second virial coefficient:
account of continuum contribution,
scattering phase shifts, Beth-Uhl.E.

Generalized Beth-Uhlenbeck
formula:
medium modified binding energies,
medium modified scattering phase shifts

chemical & physical picture

Cluster virial approach:
all bound states (clusters)
scattering phase shifts of all pairs

Correlated medium
phase space occupation by all bound states
in-medium correlations,
quantum condensates

Cluster virial expansion for nuclear matter within a quasiparticle approach

Generalized Beth-Uhlenbeck approach

$$n_1^{\mathrm{qu}}(T,\mu_p,\mu_n) = \sum_{A,Z,\nu} \frac{A}{\Omega} \sum_{\substack{\vec{P} \\ P>P_{\mathrm{Mott}}}} f_A\big(E_{A,Z,\nu}(\vec{P};T,\mu_p,\mu_n),\mu_{A,Z,\nu}\big)$$

$$\begin{aligned} n_2^{\mathrm{qu}}(T,\mu_p,\mu_n) &= \sum_{A,Z,\nu} \sum_{A',Z',\nu'} \frac{A+A'}{\Omega} \sum_{\vec{P}} \sum_{c} g_c \frac{1+\delta_{A,Z,\nu;A',Z',\nu'}}{2\pi} \\ &\times \int_0^\infty dE\, f_{A+A'}\left(E_c(\vec{P};T,\mu_p,\mu_n)+E,\mu_{A,Z}+\mu_{A',Z'}\right) 2\sin^2(\delta_c)\,\frac{d\delta_c}{dE} \end{aligned}$$

Avoid double counting

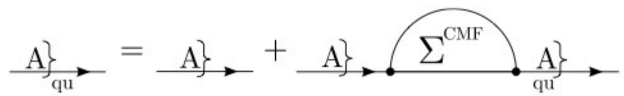

Generating functional

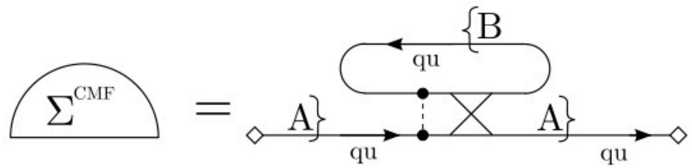

G.R., N. Bastian, D. Blaschke, T. Klaehn, S. Typel, H. Wolter, NPA **897**, 70 (2013)

Equation of state: chemical potential

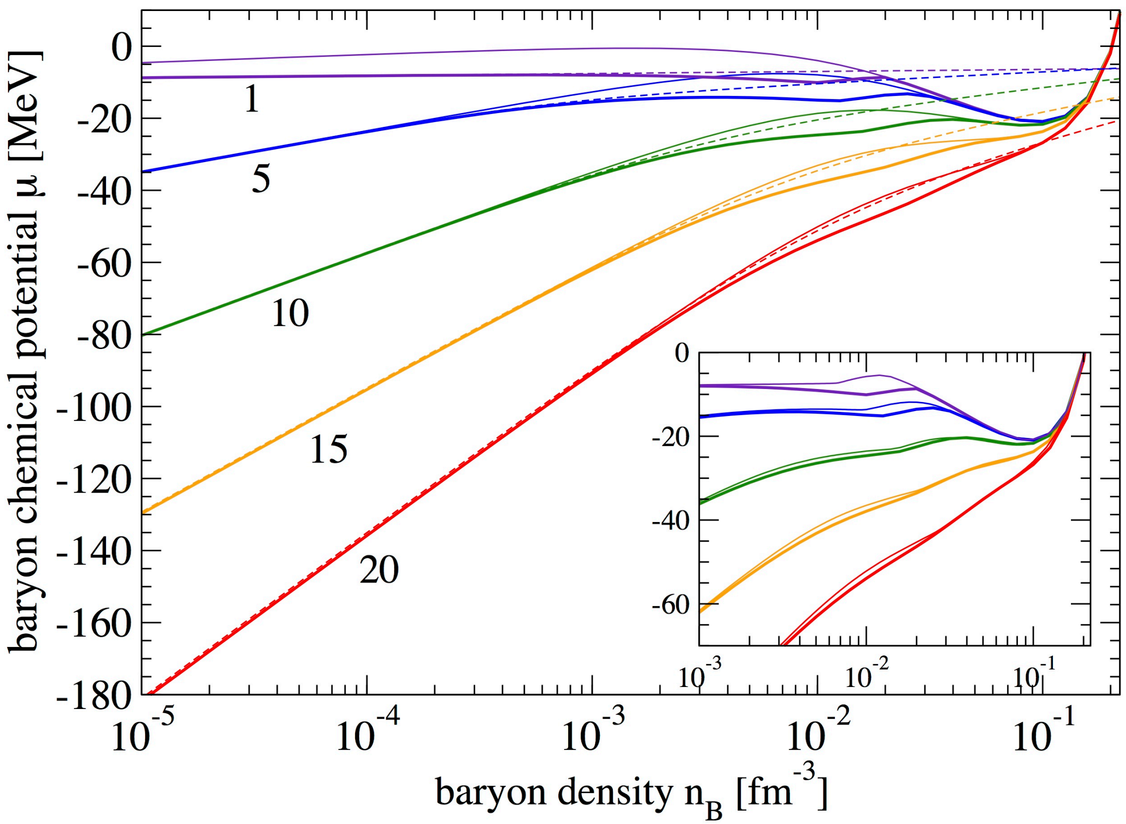

Chemical potential for symmetric matter. T=1, 5, 10, 15, 20 MeV.
QS calculation compared with RMF (thin) and NSE (dashed).
Insert: QS calculation without continuum correlations (thin lines).

Symmetric matter: free energy per nucleon

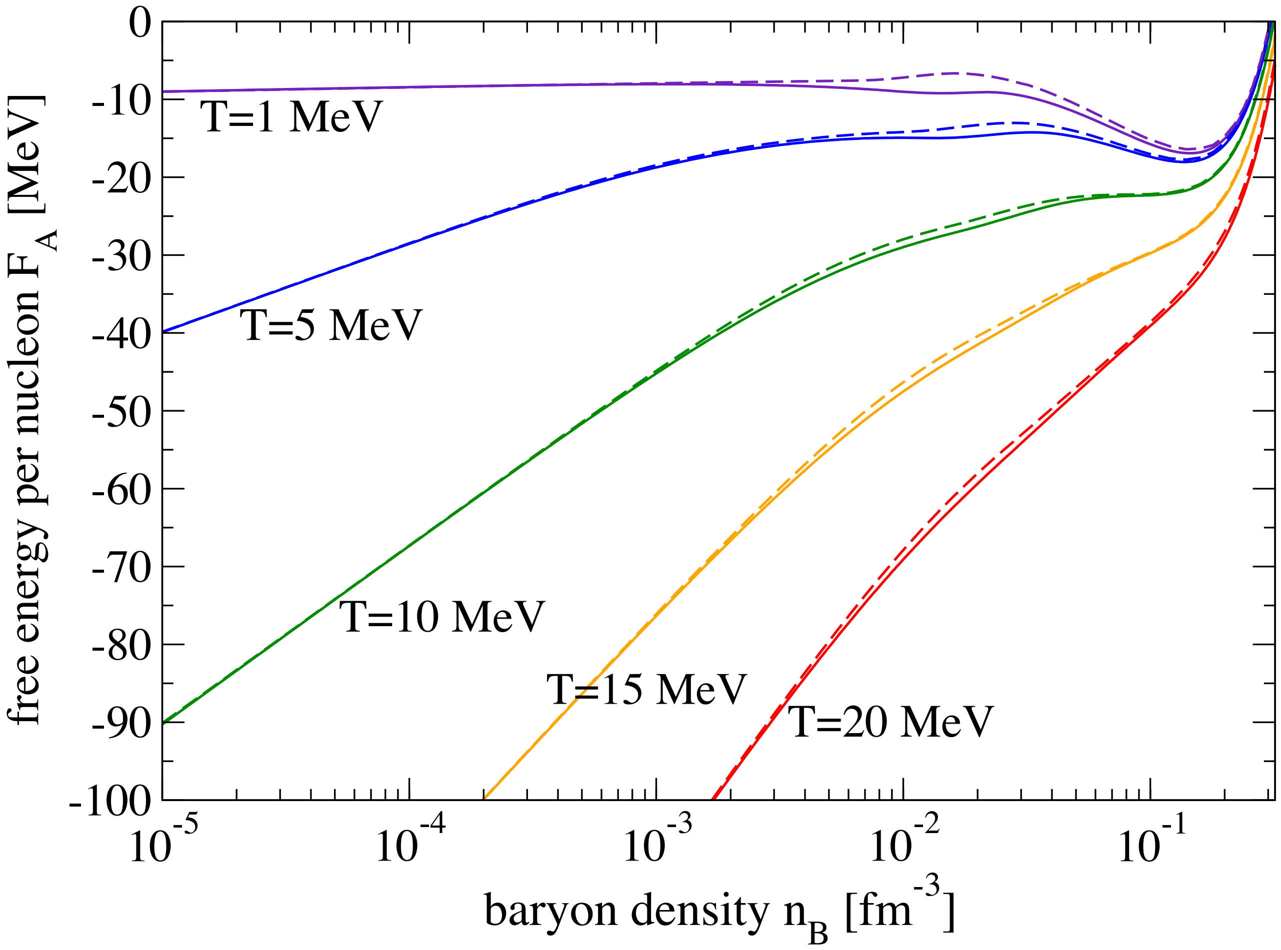

Dashed lines: no continuum correlations

G. R., PRC **92**, 054001 (2015)

Light Cluster Abundances

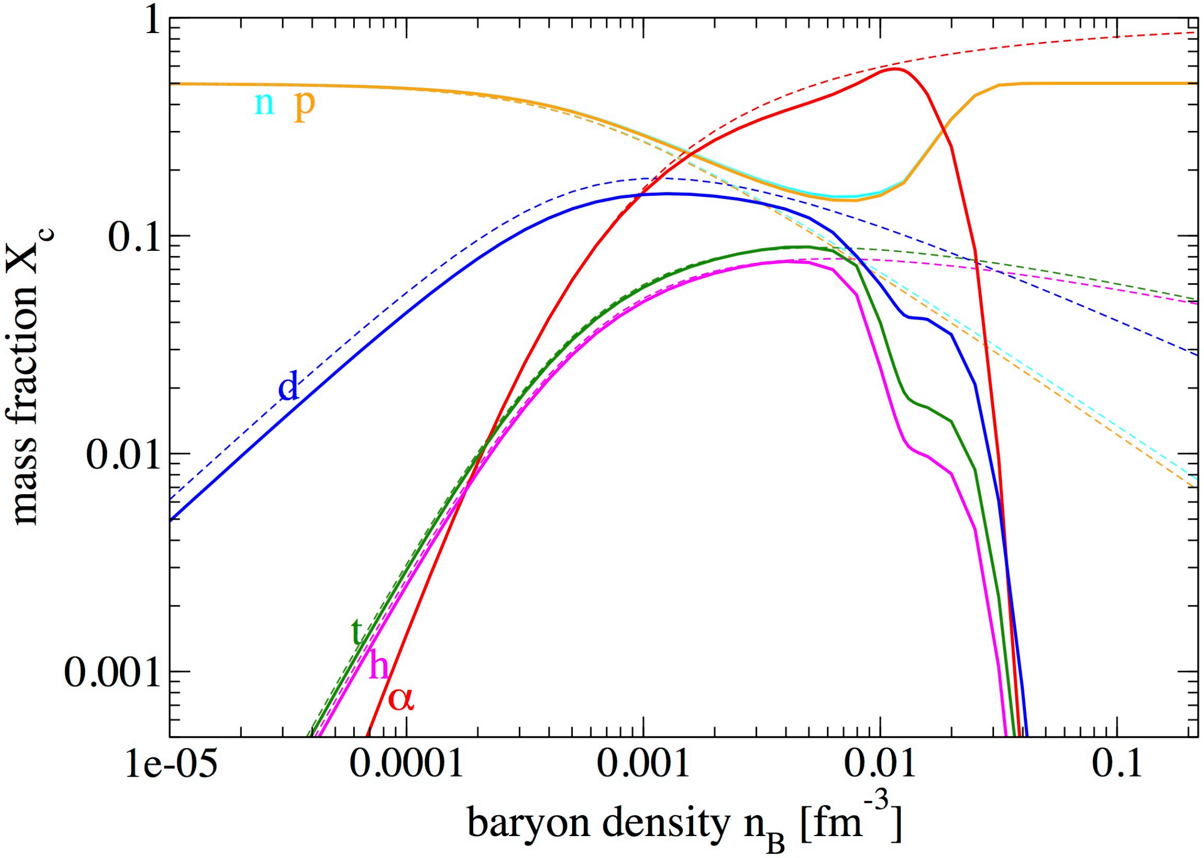

Composition of symmetric matter in dependence on the baryon density n_B, T = 5 MeV.
Quantum statistical calculation (full) compared with NSE (dotted).

G. R., PRC **92**, 054001 (2015)

Pauli blocking in symmetric matter

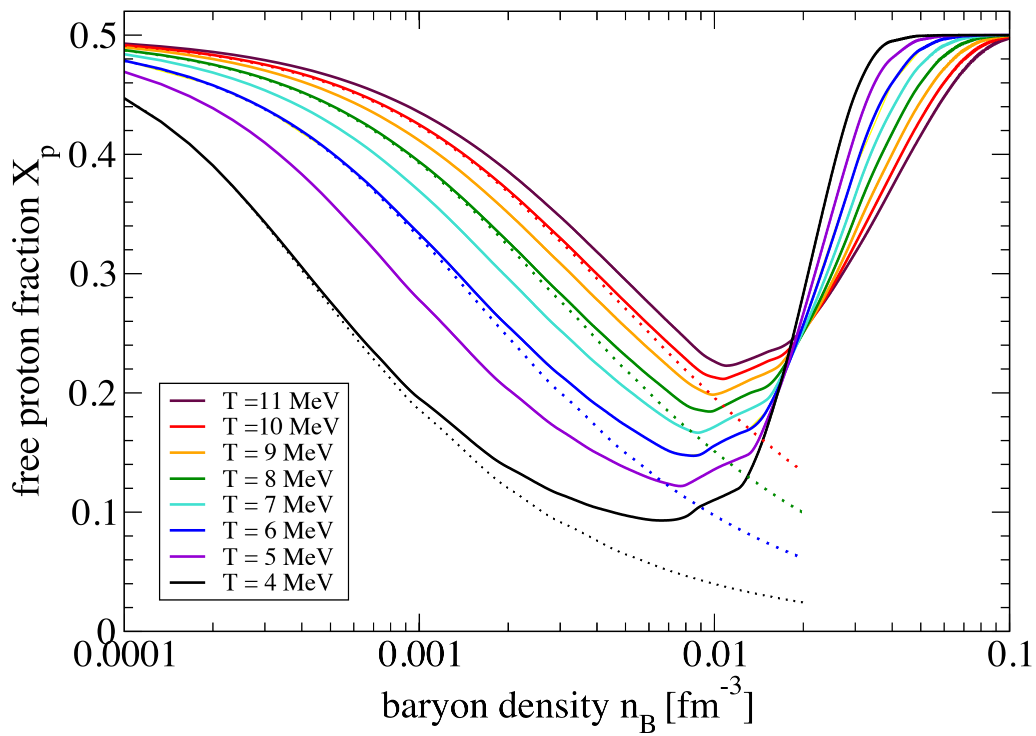

Free proton fraction as function of density and temperature in symmetric matter.
QS calculations (solid lines) are compared with the NSE results (dotted lines).
Mott effect in the region $n_{saturation}/5$.

Fermi liquid and clustering

isothermal compressibility

$$\kappa_{\mathrm{iso}}(T,\mu) = -\frac{1}{\Omega_0}\frac{\partial \Omega_0}{\partial p}\Big|_T = \frac{1}{n_B^2}\left(\frac{\partial n_B}{\partial \mu}\right)\Big|_T$$

thermodynamic potential

$$p(T,\mu) = \int_{-\infty}^{\mu} n_B(T,\mu')d\mu'$$

incompressibility

$$K(T,n_B) = \frac{1}{n_B \kappa_{\mathrm{iso}}} = n_B \frac{\partial \mu}{\partial n_B}\Big|_T$$

Dynamic structure factor

baryon density $\hat{n}_B(\mathbf{r}) = \sum_\nu \psi_\nu^\dagger(\mathbf{r})\psi_\nu(\mathbf{r})$

wave number dependent density fluctuation

$$\rho_{\mathbf{q}} = \int d^3r\, e^{i\mathbf{q}\cdot\mathbf{r}} \sum_\nu \psi_\nu^\dagger(\mathbf{r})\psi_\nu(\mathbf{r})$$

$$S(\mathbf{q},\omega) = \frac{1}{2\pi\Omega_0}\int_{-\infty}^{\infty} dt \langle \rho_{\mathbf{q}}^{+}(t)\rho_{\mathbf{q}}(0)\rangle e^{i\omega t}$$

static structure factor

$$S(\mathbf{q}) = \int d\omega\, S(\mathbf{q},\omega)$$

incompressibility

$$S(\mathbf{q}\to 0) = (\langle \hat{n}_B^2(\mathbf{r})\rangle - n_B^2)/n_B = T/\left(\frac{\partial\mu}{\partial n_B}\right)\Big|_T$$

response function χ(q, ω)

$$\langle \rho_{\mathbf{q}}(\omega) \rangle = \chi(\mathbf{q}, \omega) U(\mathbf{q}, \omega)$$

thermodynamic density-density Green function

$$L(1,2;1^+,2^+) = \frac{\Omega_0}{\mathrm{i}^2} \langle \mathrm{T}\{\psi^\dagger(1^+)\psi(1)\psi^\dagger(2^+)\psi(2)\}\rangle - \frac{\Omega_0}{\mathrm{i}^2} \langle \psi^+(1^+)\psi(1)\rangle \langle \psi^+(2^+)\psi(2)\rangle$$

$$1 = \{\mathbf{r}_1, \tau_1, \nu_1\}$$

fluctuation-dissipation theorem

$$\mathrm{Im}\chi(\mathbf{q}, \omega) = -\mathrm{Im}L(\mathbf{q}, \omega - \mathrm{i}0)$$

$$S(\mathbf{q}, \omega) = \frac{1}{\pi} \frac{1}{e^{\beta\omega} - 1} \mathrm{Im}L(\mathbf{q}, \omega - \mathrm{i}0)$$

$$\kappa_{\mathrm{iso}}(T, \mu) = \frac{\beta}{n_B^2} \lim_{\mathbf{q}\to 0} \int_{-\infty}^{\infty} \frac{d\omega}{\pi} \frac{1}{e^{\beta\omega} - 1} \mathrm{Im}L(\mathbf{q}, \omega - \mathrm{i}0)$$

Approximations

Matsubara Green function

$$L(\mathbf{q}, z_\lambda) = \int d^3r \int_0^\beta d\tau e^{\mathrm{i}\mathbf{q}\cdot(\mathbf{r}_2-\mathbf{r}_1)} e^{\mathrm{i}z_\lambda(\tau_2-\tau_1)} L(1,2;1^+,2^+)$$

$$z_\lambda = \pi\lambda/\beta,\ \lambda = 0,\ \pm 2, \ldots$$

Feynman diagrams

real time non-equilibrium Green functions

$$-\mathrm{i}\Pi^{\mu\nu}_{-+}(q;X) = {}^{+}\boxed{-\mathrm{i}\boldsymbol{\Pi}}^{-} = \int \mathrm{d}^4\xi e^{\mathrm{i}q\xi} \langle j^{\mu\dagger}(X-\xi/2) j^{\nu}(X+\xi/2)\rangle$$

Noninteracting Fermi-gas

polarization loop

$$L(\vec{q},\omega_\mu) \approx \Pi_1^0(\vec{q},\omega_\mu) \;=$$

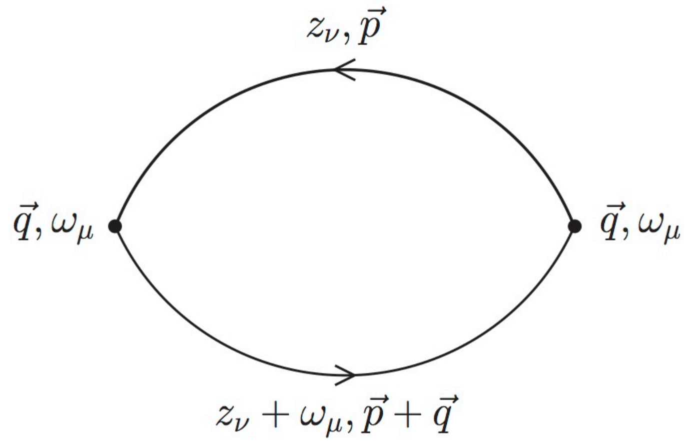

$$L_0(\mathbf{q}, z) = g_\nu \int \frac{d^3p}{(2\pi)^3} \frac{f^0_{\mathbf{p}} - f^0_{\mathbf{p}+\mathbf{q}}}{z + \epsilon^0_{\mathbf{p}} - \epsilon^0_{\mathbf{p}+\mathbf{q}}}$$

$$S_0(\mathbf{q}, \omega) = \frac{1}{e^{\beta\omega} - 1} g_\nu \int \frac{d^3p}{(2\pi)^3} \left(f^0_{\mathbf{p}} - f^0_{\mathbf{p}+\mathbf{q}}\right) \delta(\omega + \epsilon^0_{\mathbf{p}} - \epsilon^0_{\mathbf{p}+\mathbf{q}})$$

isothermal compressibility

$$\kappa^{(0)}_{\text{iso}}(T, \mu) = \frac{\beta}{n_B^2} g_\nu \int \frac{d^3p}{(2\pi)^3} f^0_p (1 - f^0_p)$$

$$n_B^{(0)}(\beta, \mu) = \frac{1}{\Omega_0} \sum_p \frac{1}{e^{\beta(\epsilon^0_p - \mu)} + 1} = \frac{1}{\Omega_0} \sum_p f^0_p = \frac{N}{\Omega_0}$$

Quasiparticle approximation

Hartree-Fock approximation

$$\epsilon_p^{\mathrm{HF}} = \epsilon_p^0 + \sum_k V(\mathbf{p}, \mathbf{k}; \mathbf{p}, \mathbf{k})_{\mathrm{ex}} f(\epsilon_k^{\mathrm{HF}})$$

$$n_B^{\mathrm{HF}}(\beta, \mu) = g_\nu \int \frac{d^3p}{(2\pi)^3} \frac{1}{e^{\beta(\epsilon_p^{\mathrm{HF}} - \mu)} + 1}$$

$$\left.\frac{\partial \mu^{\mathrm{HF}}}{\partial n_B}\right|_T = \left\{ \frac{g_\nu}{2\pi^2} \int_0^\infty p^2 dp f_p^{\mathrm{HF}} (1 - f_p^{\mathrm{HF}}) \beta \left[1 - \beta \int \frac{d^3k}{(2\pi)^3} V(\mathbf{p}, ; \mathbf{p}, \mathbf{k})_{\mathrm{ex}} f_k^{\mathrm{HF}} (1 - f_k^{\mathrm{HF}}) \right] \right\}^{-1}$$

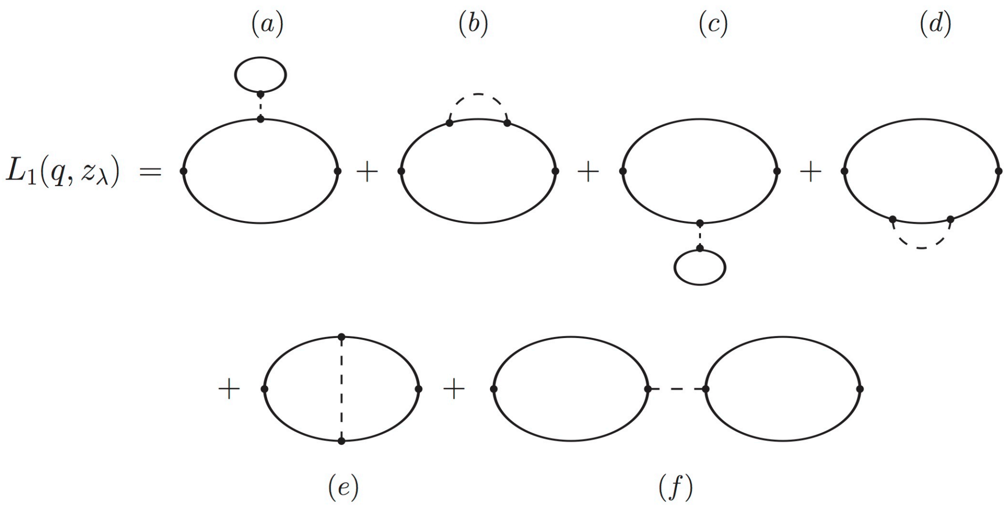

$$\kappa_{\mathrm{iso}}^{(1)}(T, \mu) = \frac{\beta}{n_B^2} g_\nu \int \frac{d^3p}{(2\pi)^3} f_p^{\mathrm{HF}} (1 - f_p^{\mathrm{HF}}) \left[1 - \beta \int \frac{d^3k}{(2\pi)^3} V(\mathbf{p}, \mathbf{k}; \mathbf{p}, \mathbf{k})_{\mathrm{ex}} f_k^{\mathrm{HF}} (1 - f_k^{\mathrm{HF}}) \right]$$

Two-particle correlations

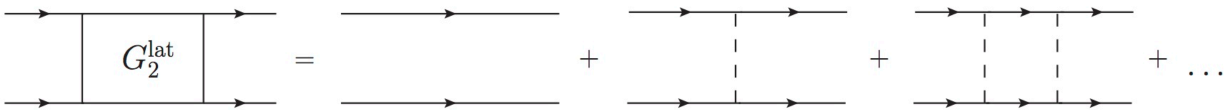

cluster propagator

$$\langle \nu, \mathbf{P} | G_2(z) | \nu', \mathbf{P}' \rangle = \frac{1}{z - E^0_{\nu,P}} \delta_{\nu\nu'} \delta_{\mathbf{P},\mathbf{P}'}$$

cluster decomposition of the self-energy

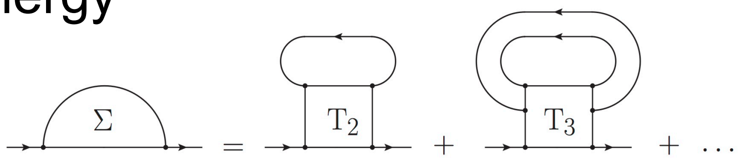

Beth-Uhlenbeck formel

$$n_B^{\mathrm{BU}}(\beta,\mu) = \frac{1}{\Omega_0} \sum_{\mathbf{p}} f_p^0 + \frac{2}{\Omega_0} \sum_{\alpha,\mathbf{P}} \int_{-\infty}^{\infty} \frac{dE_{\mathrm{rel}}}{\pi} f_2 \left(E_{\mathrm{rel}} + \frac{P^2}{4m} \right) D^{\mathrm{BU}}_{\alpha,\mathbf{P}}(E_{\mathrm{rel}}),$$

$$D^{\mathrm{BU}}_{\alpha,\mathbf{P}}(E_{\mathrm{rel}}) = g_\alpha \left(\sum_{\nu} \pi \delta(E_{\mathrm{rel}} - E^0_{\alpha\nu,\mathbf{P}}) + \frac{\partial}{\partial E_{\mathrm{rel}}} \delta_{\alpha,\mathbf{P}}(E_{\mathrm{rel}}) \right)$$

Cluster decomposition of the polarization function

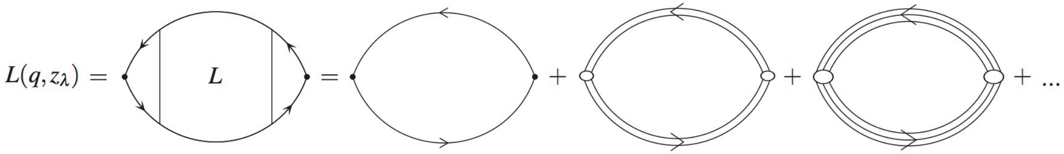

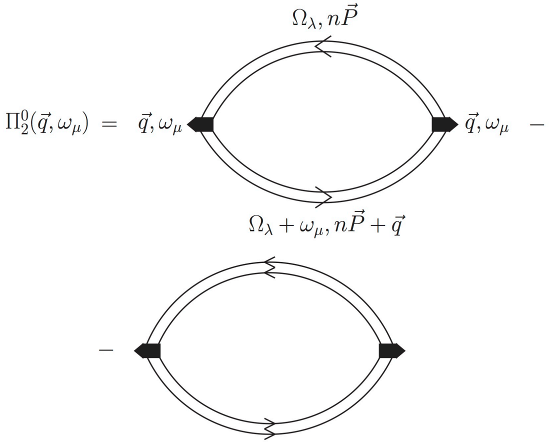

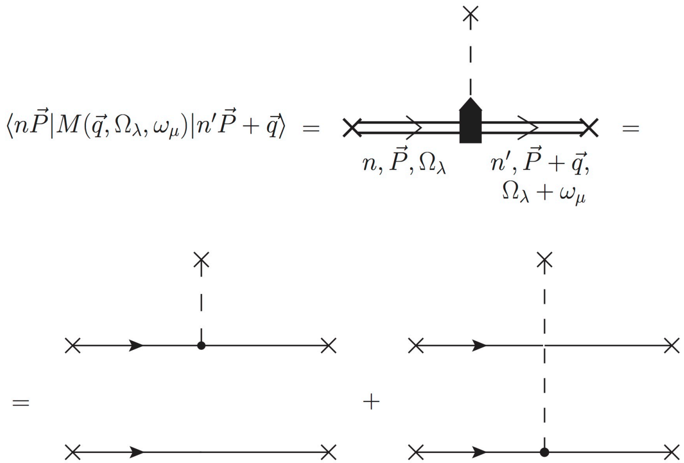

$$M_{\nu\nu'}(\mathbf{q}) = \langle \nu, \mathbf{P}|M(\mathbf{q}, z_\lambda, z_\mu)|\nu', \mathbf{P} + \mathbf{q}\rangle = \sum_{\mathbf{p}_1, \mathbf{p}_2} \psi^*_{\nu, \mathbf{P}}(p_1, p_2)[\psi_{\nu', \mathbf{P}+\mathbf{q}}(\mathbf{p}_1 + \mathbf{q}, \mathbf{p}_2) + \psi_{\nu', \mathbf{P}+\mathbf{q}}(\mathbf{p}_1, \mathbf{p}_2 + \mathbf{q})]$$

$$\kappa_{\text{iso}}^{(\text{BU})}(T, \mu_n, \mu_p) = \frac{\beta}{\Omega_0 n_B^2} \left\{ \sum_{\mathbf{p}} f_p^0(1 - f_p^0) + \sum_{\alpha, \mathbf{P}} \int_{-\infty}^{\infty} \frac{dE}{\pi} f_2\left(E + \frac{P^2}{4m}\right) \left[1 + f_2\left(E + \frac{P^2}{4m}\right)\right] D_{\alpha, \mathbf{P}}(E) \right\}$$

Heavier clusters?

In principle, clusters with arbitrary A should be considered.

Clusters with 4 < A <12 : weakly bound, no significant contributions

Heavy clusters: Thomas-Fermi model,

Region of thermodynamic instability: Pasta structures

$$\Delta E_{A\nu P}(n_B) = \sum_{\tau=n,p} \int d^3r \Delta E_\tau^{\rm SE}(n_n^A(r), n_p^A(r)) n_\tau \times \int_{\Lambda_\tau p_F(n_\tau^A(r))}^{\infty} \frac{y dy}{2\pi x_\tau} \left[e^{-(y-x_\tau)^2/4\pi} - e^{-(y+x_\tau)^2/4\pi} \right]$$

$$n_B^A(r) = \frac{3A}{4\pi R^3} \frac{1}{1+(\pi b/R)^2} \left[\frac{1}{1+e^{(r-R)/b}} + \frac{1}{1+e^{(-r-R)/b}} \right]$$

V.V. Burov, Yu.N. Eldyshev, V.K. Lukyanov, and Yu.S. Pol, Dubna-preprint E4-8029, Joint Institute for Nuclear Research, Dubna 1974.

Light Clusters and Pasta Phases in Warm and Dense Nuclear Matter

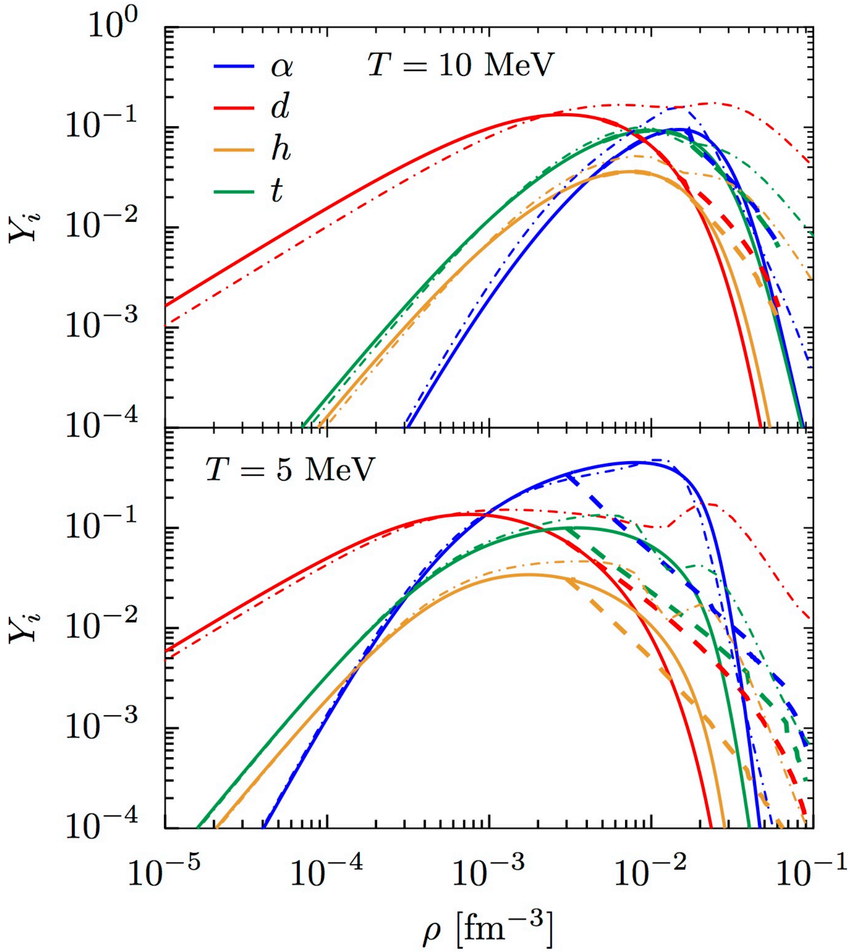

FIG. 7. Cluster fractions with $\eta = 0.70$ and $Y_p = 0.41$ as a function of density, for $T = 5$ MeV (bottom) and $T = 10$ MeV (top panels). Results for a TF calculation (dashed), homogeneous matter with clusters (solid), and the QS approach (dash-dotted lines) are shown. For $T = 5$ MeV, the TF calculation includes the five geometrical configurations, droplet, rod, slab, tube and bubble, for the heavy clusters.

Sidney S. Avancini et al., arXiv:1704.00054

Light Clusters and Pasta Phases in Warm and Dense Nuclear Matter

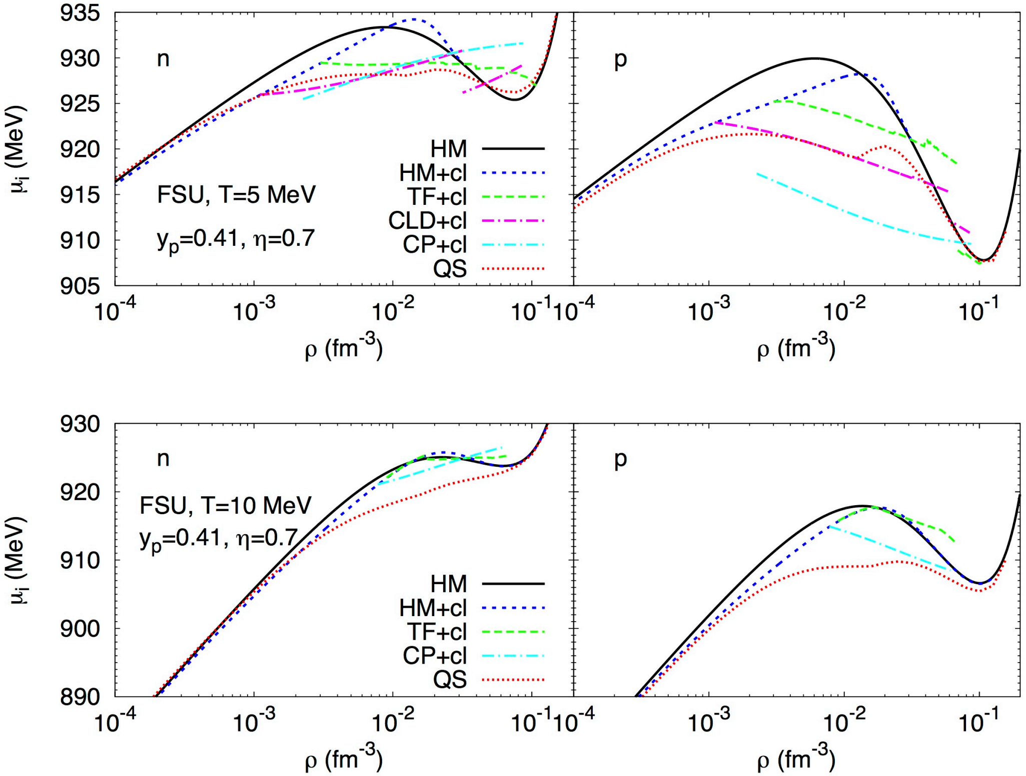

Sidney S. Avancini et al., arXiv:1704.00054

FIG. 8. Neutron (left panels) and proton (right panels) chemical potentials with $\eta = 0.7$ and $Y_p = 0.41$ as a function of density at $T = 5$ MeV (top) and $T = 10$ MeV (bottom), for homogeneous nuclear matter (HM) (solid), nuclear matter with light clusters (blue short-dashed), and mean-field pasta calculations with clusters [TF (green, dashed), CLD (pink, dash-dotted), CP (cyan, dash-dotted)]. QS results (red, dotted) are also shown.

Light clusters and pasta phases in core-collapse supernova matter

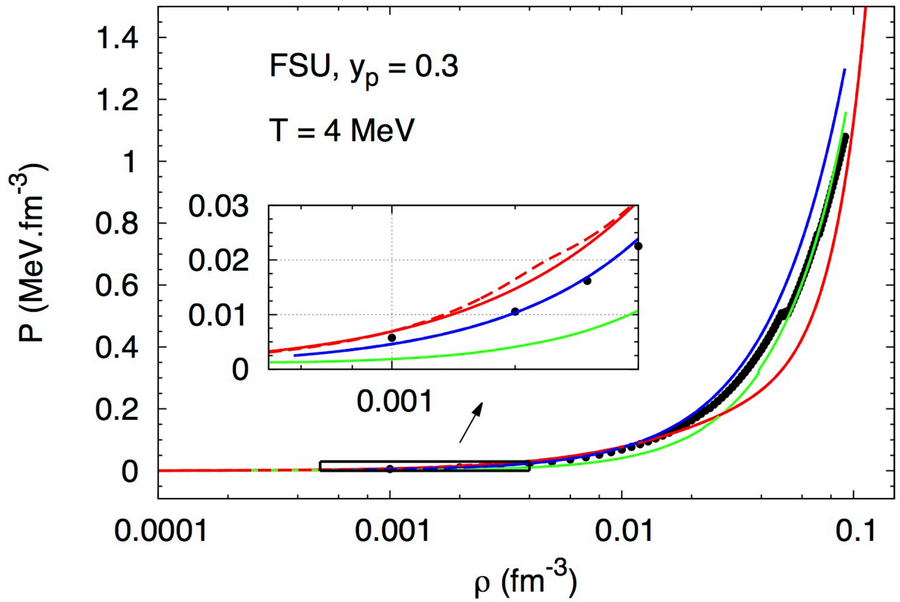

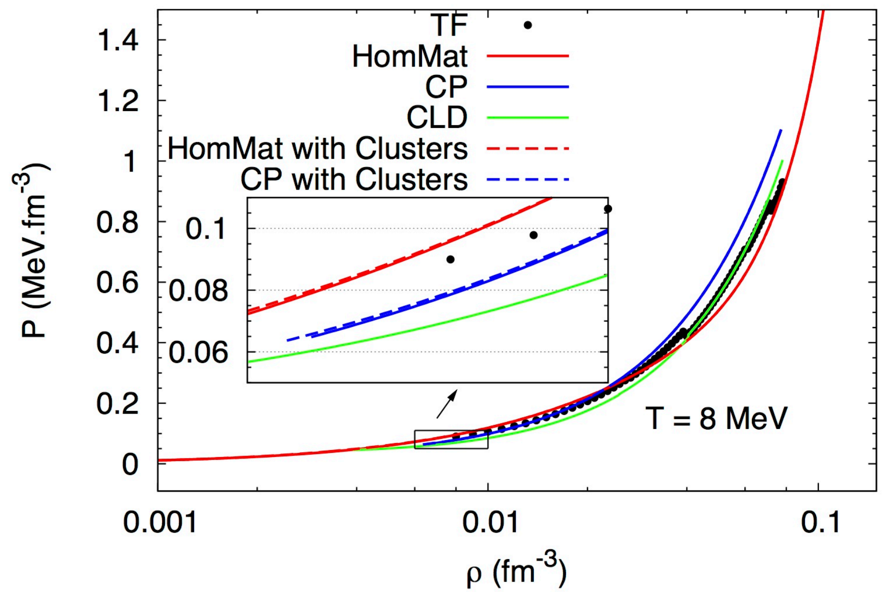

Pressure as function of density, Yp=0.3, T=4 MeV / 8 MeV.
With and without pasta, including or not clusters. TF - Thomas-Fermi, CP – coexisting-phases method, CLD – compressible liquid drop

H. Pais, S. Chiacchiera, C. Providencia, PRC **91**, 055801 (2015)

Nuclear matter phase diagram

Core collapse supernovae

Thermodynamic parameters:

baryon density n_B

temperature T

electron fraction Y_e

T. Fischer et al., ApJS 194, 39 (2011)

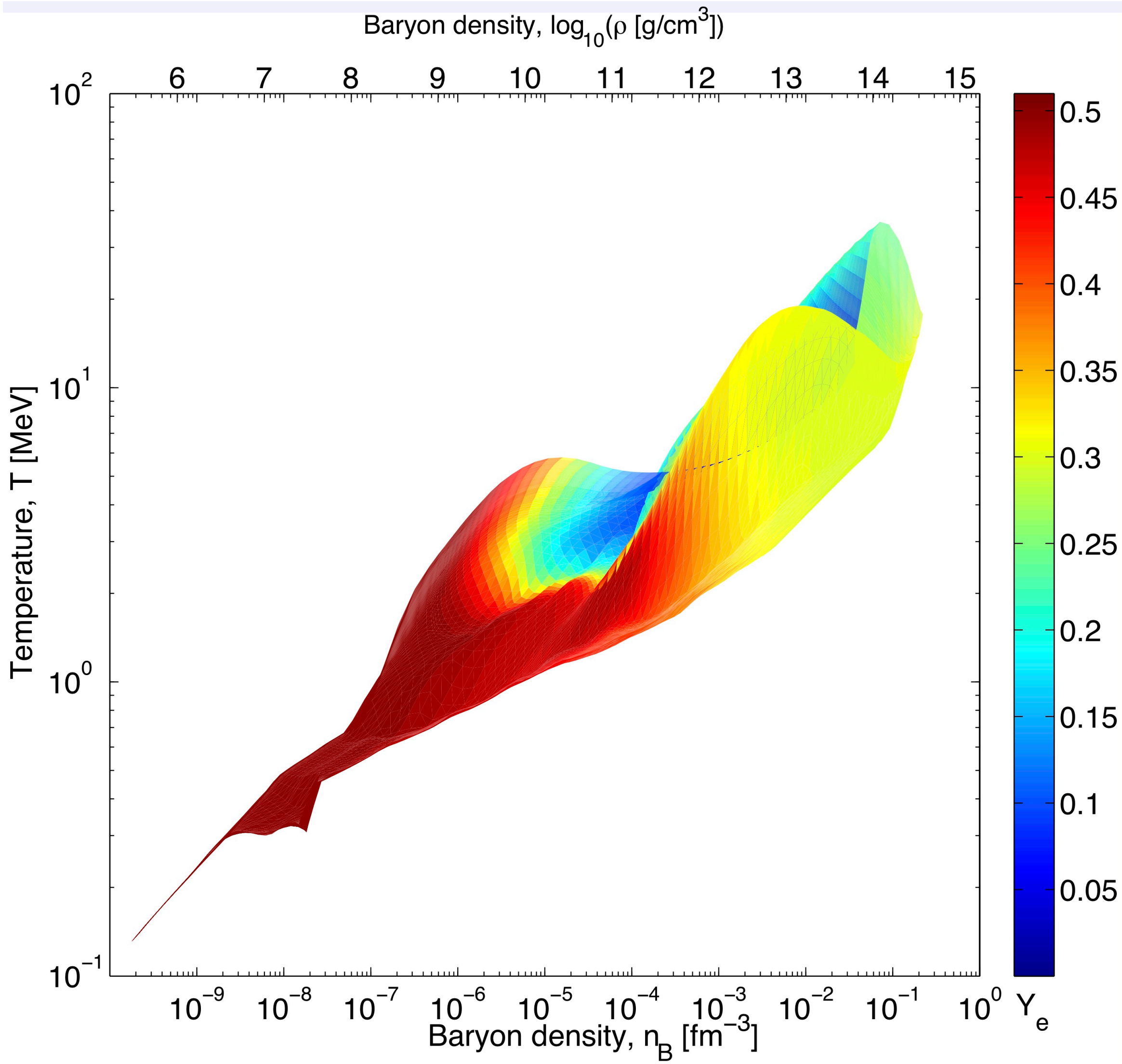

Nuclear matter phase diagram

Exploding supernova

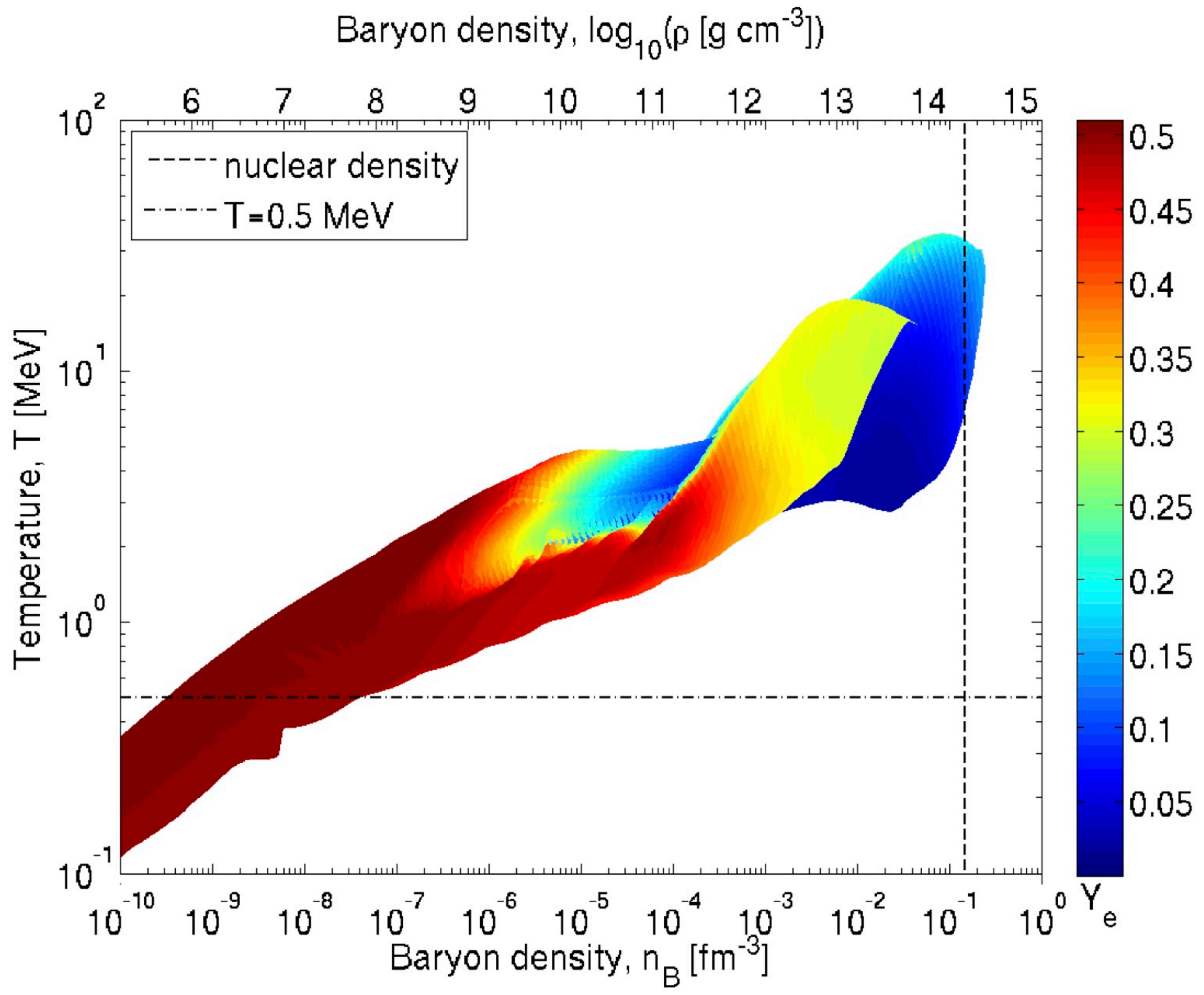

T. Fischer et al., arXiv 1307.6190

Neutron star masses

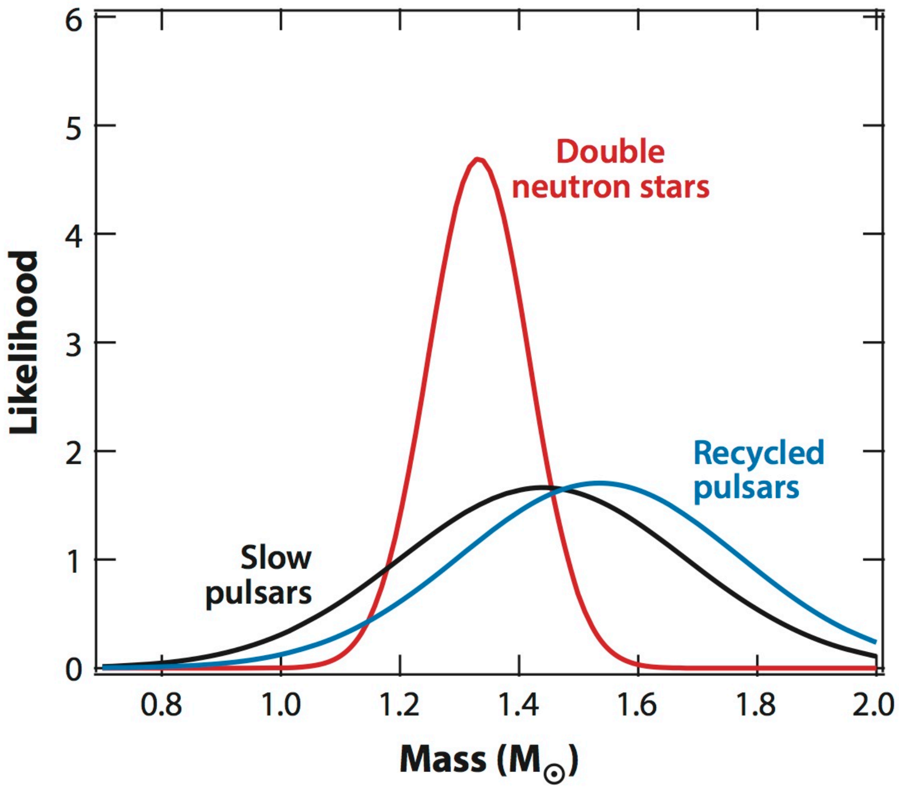

inferred mass distributions
for the different populations of neutron stars.

F. Ozel and P. Freire, Annu. Rev. Astron. Astrophys. **54**, 401 (2016)

Neutron star radii

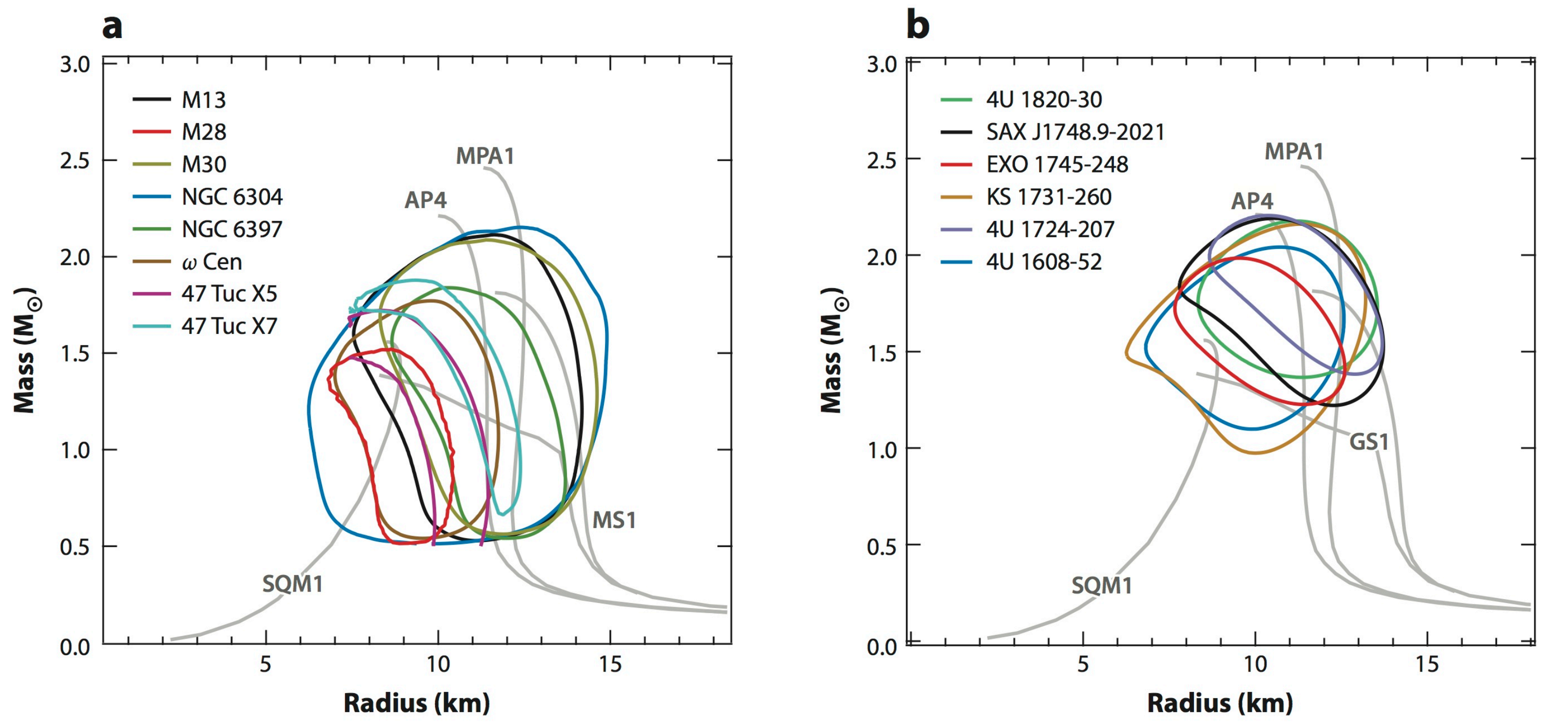

Figure 4

The combined constraints at the 68% C.L. over the neutron-star mass and radius obtained from (*a*) all neutron stars in low-mass X-ray binaries during quiescence and (*b*) all neutron stars with thermonuclear bursts. The light gray lines show mass relations corresponding to a few representative EoSs (see Section 4.1 and **Figure 7** for detailed descriptions and the naming conventions for all equations of state).

F. Ozel and P. Freire, Annu. Rev. Astron. Astrophys. **54**, 401 (2016)

Neutron star radii

mass – radius relation for neutron stars: observation and theories

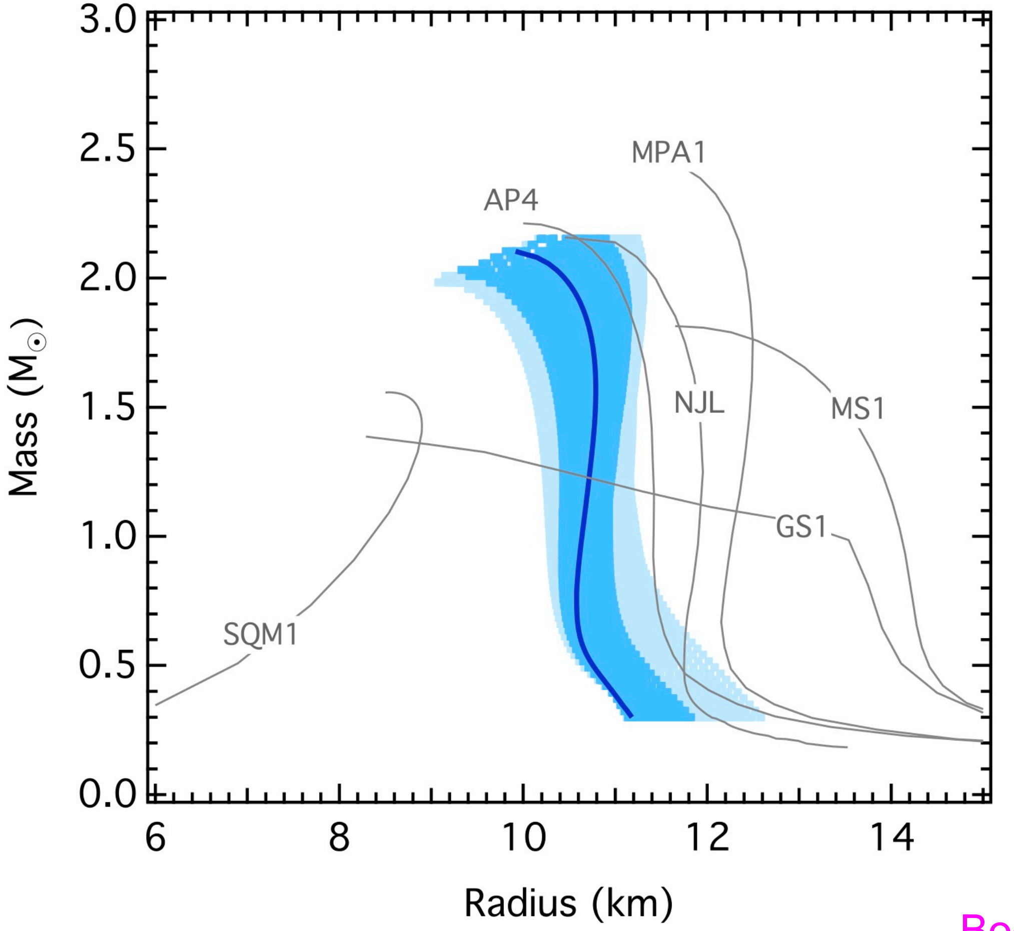

Chandra,
NICER
(Neutron-star Interior
Composition Explorer)

X7, X5 in 47 Tuc
9.9 – 11.2 km for
$M/M_\odot$ = 1.5

Bogdanov et al., Ap. J. **831**, 184 (2016)

Mass – radius relation

(a)

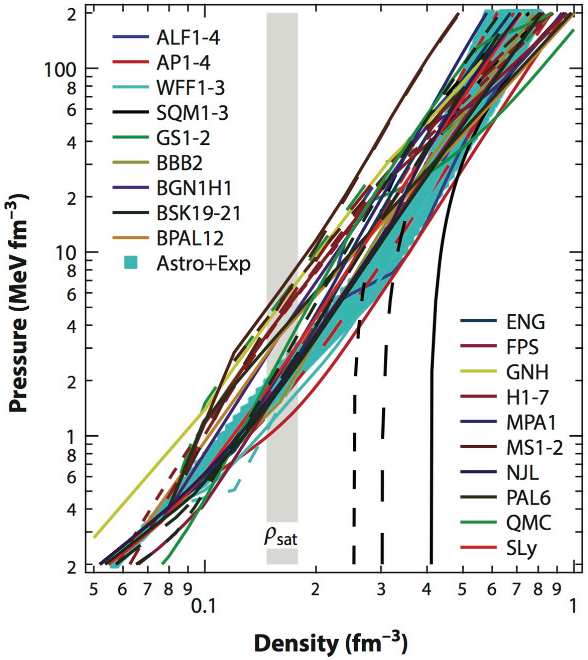

(b)

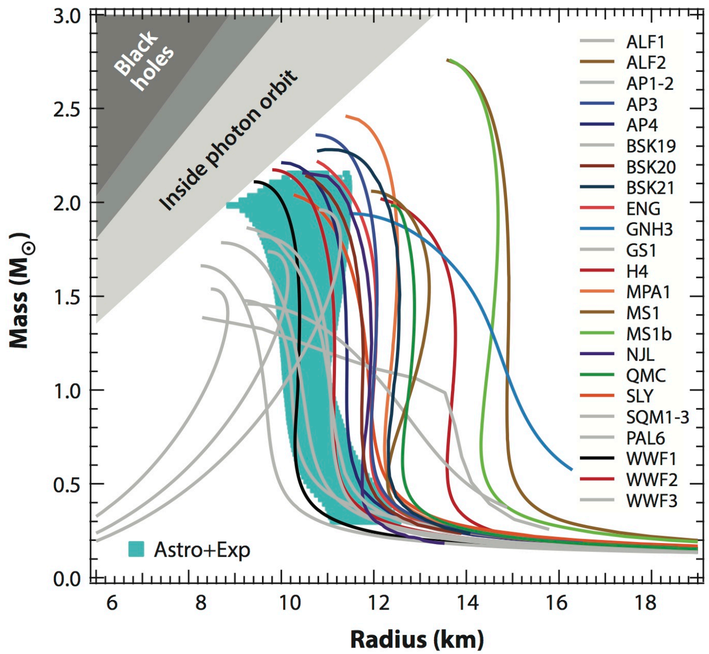

The astrophysically inferred (a) EoS and (b) mass-radius (M-R) relation corresponding to the most likely triplets of pressures that agree with all of the neutron-star radius and low-energy nucleon–nucleon scattering data and allow for an M > 1.97-$M_\odot$ neutron-star mass.

The light blue bands show the range of pressures and the M-R relations that correspond to the region of the (P1, *P2, P3)* parameter space in which the likelihood is within *e−1* of its highest value. Around 1.5 $M_\odot$, this inferred EoS predicts radii in the range of 9.9–11.2 km

F. Ozel and P. Freire, Annu. Rev. Astron. Astrophys. 54, 401 (2016)

Neutron matter, RMF-DD2

consistent equations of state: pressure and internal energy density

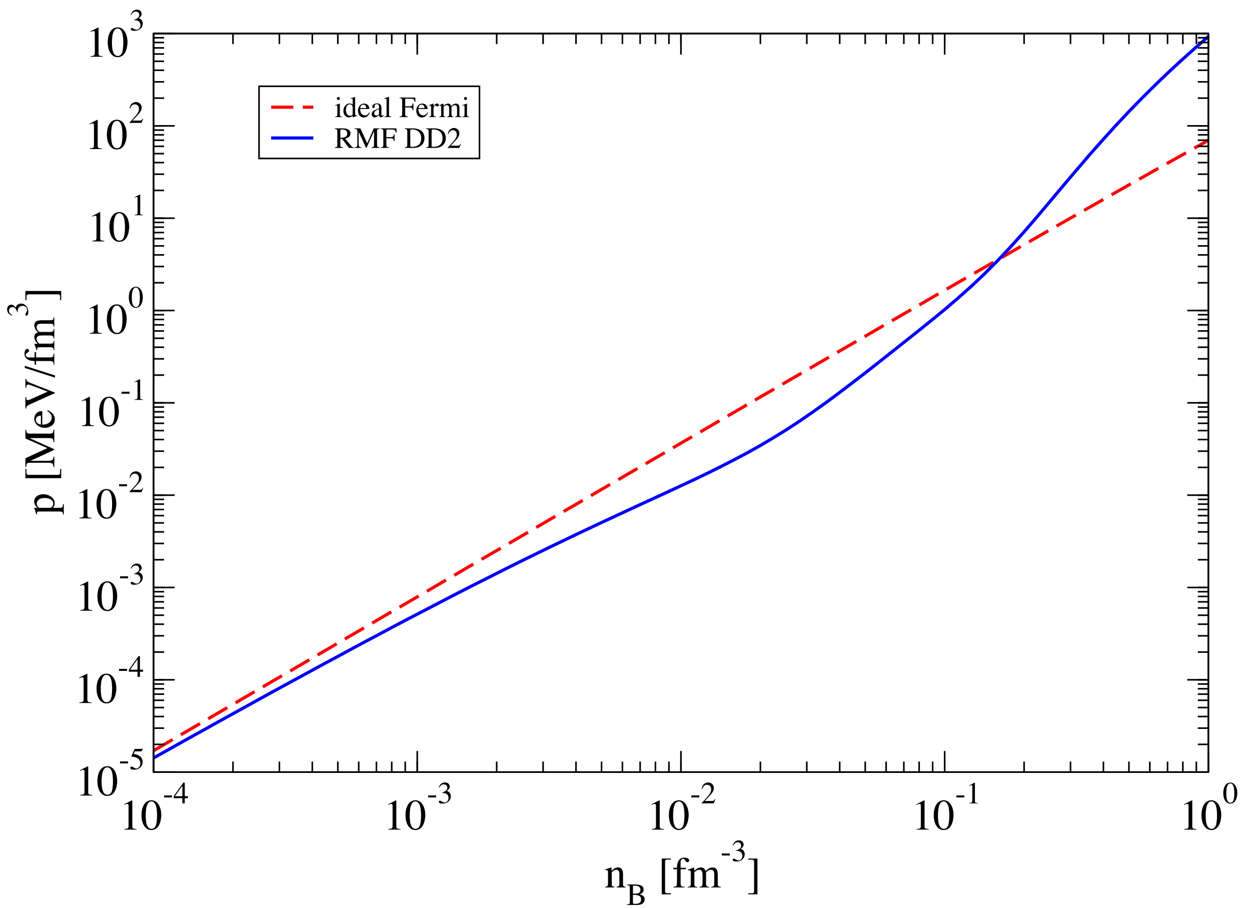

Neutron matter, RMF-DD2

solution of the TOV equations for different central density

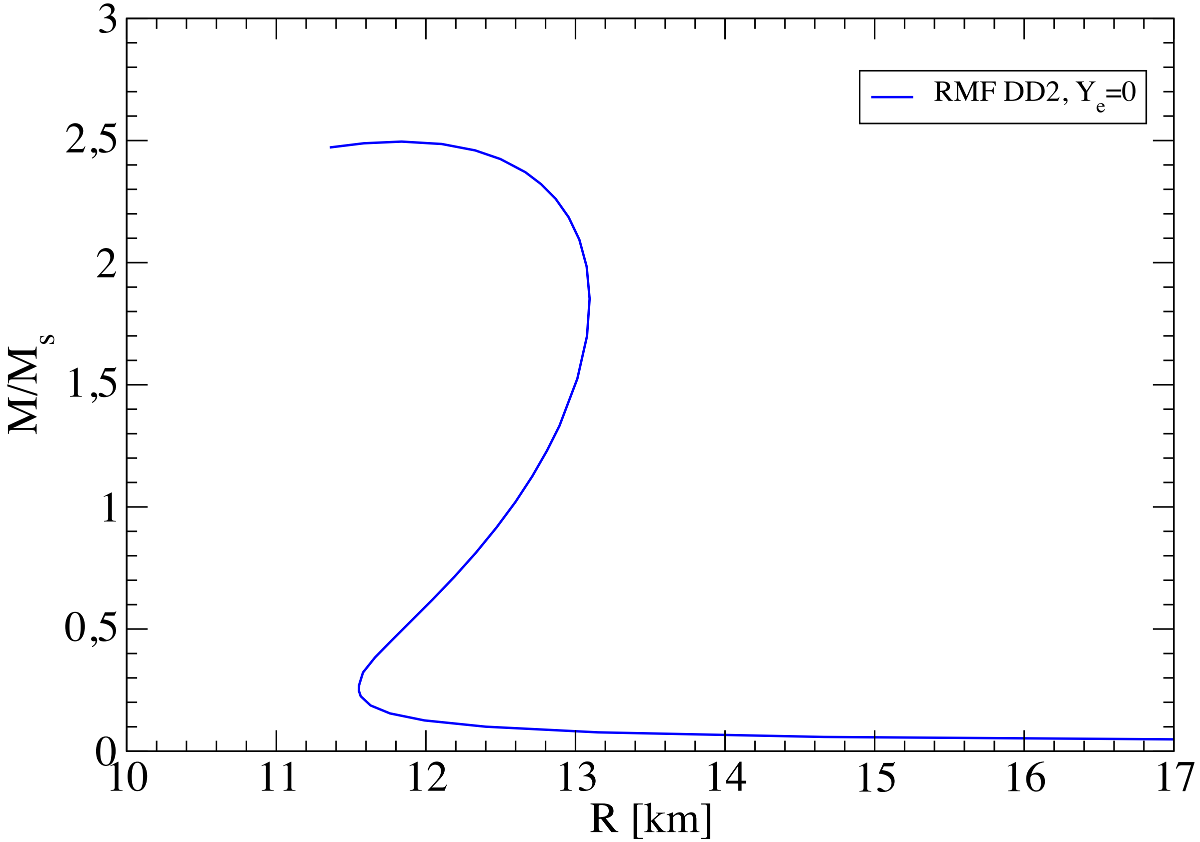

Density of neutron star crust

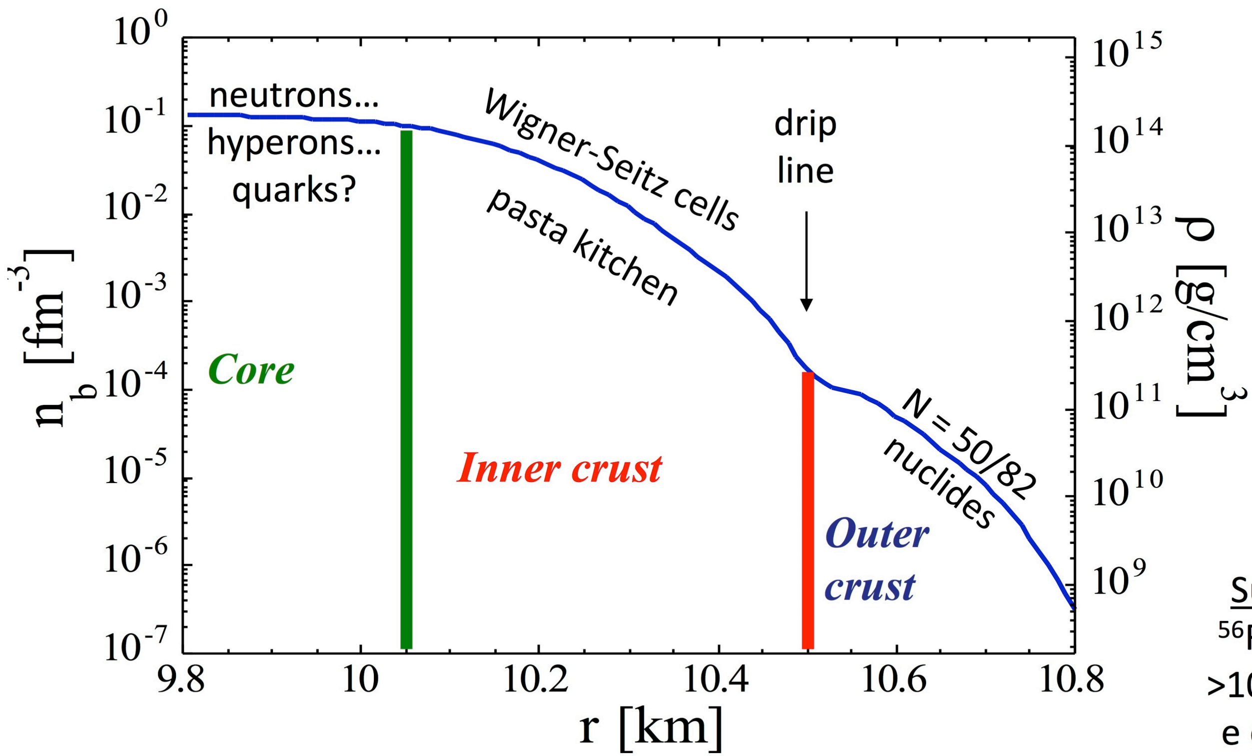

Surface:
^{56}Fe; ^{62}Ni;
$>10^7$ g/cm^3
e degen.:
$p + e \rightarrow n$

J. M. Pearson *et al.*, PRC **83**, 065810 (2011)

Heavy clusters

low density region

nuclei (Fe, Ni)

screening of the
Coulomb repulsion:
Debye
Wigner-Seitz cell

large neutron numbers
at increasing density

outer crust

until neutron drip:
unbound neutrons

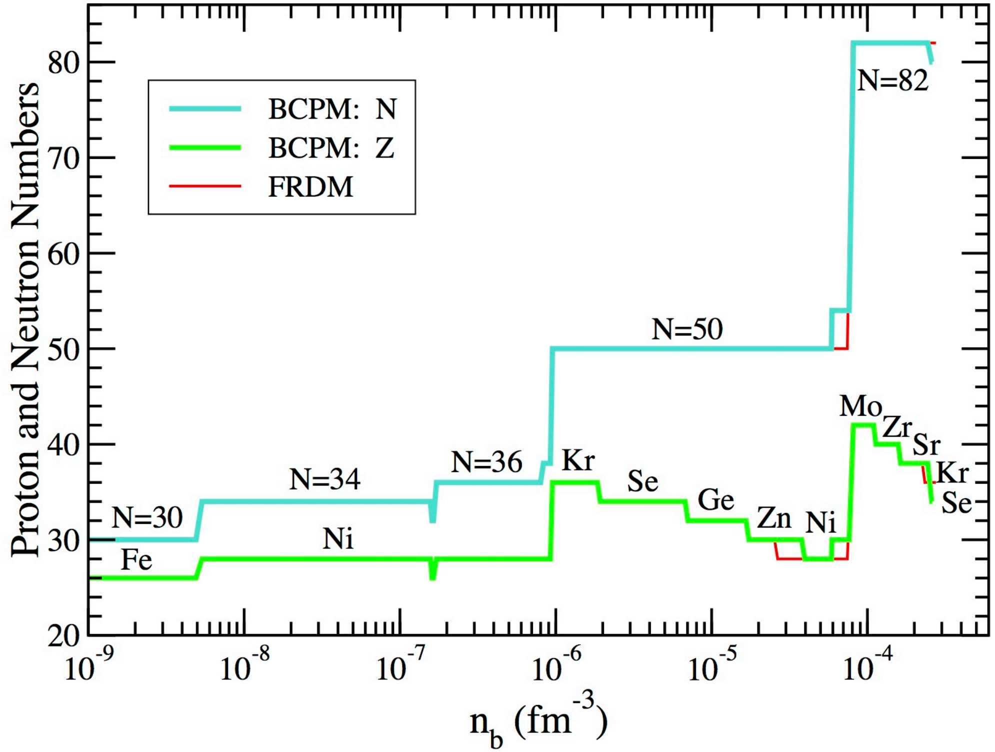

Fig. 1. Neutron (N) and proton (Z) numbers of the predicted nuclei in the outer crust of a neutron star using the experimental nuclear masses (Audi et al. 2012; Wolf et al. 2013) when available and the BCPM energy density functional or the FRDM mass formula (Möller et al. 1995) for the unmeasured masses.

B. K. Sharma et al., arxiv: 1506.00375

EOS, outer crust

low density:
heavy nuclei

pressure
as function
of density

neutron drip:
$n_B = 2.62 \times 10^{-4}\ fm^{-3}$

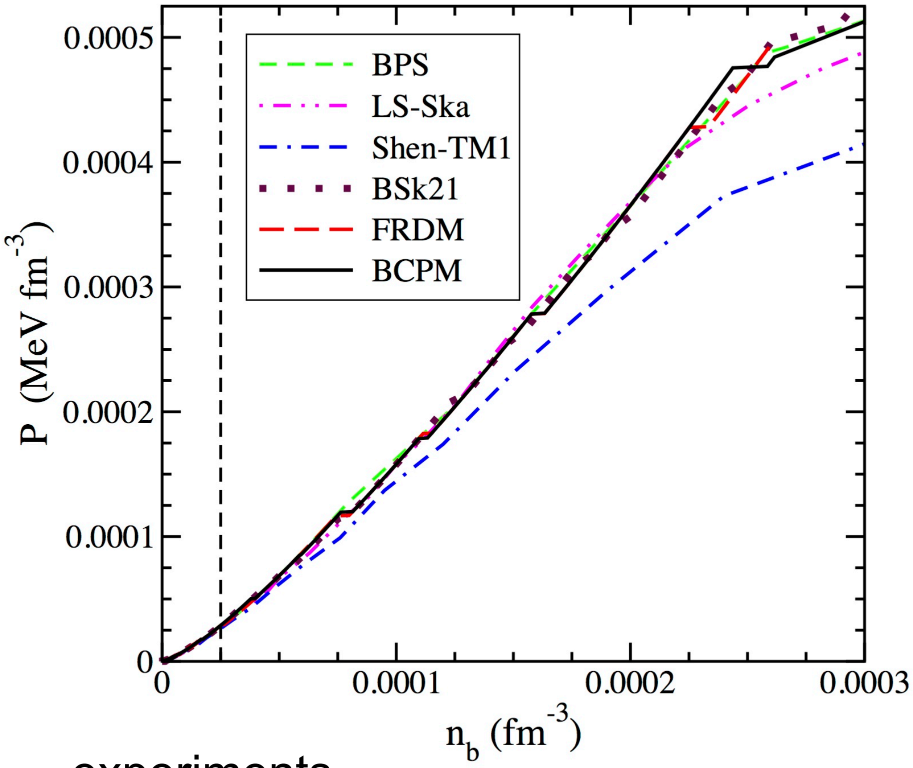

experiments

B. K. Sharma et al., arxiv: 1506.00375

Inner crust: pasta structures

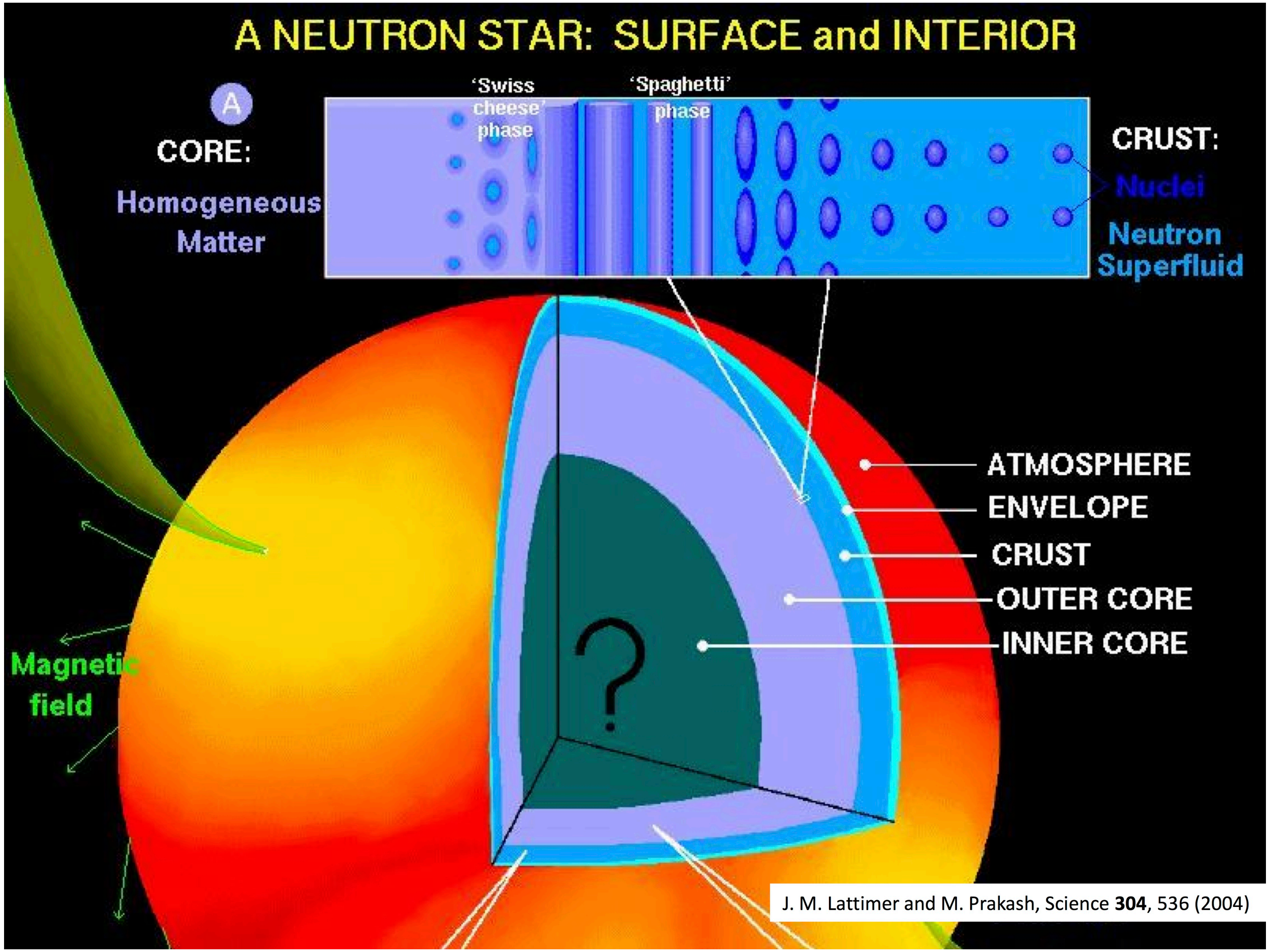

J. M. Lattimer and M. Prakash, Science **304**, 536 (2004)

EoS: inner crust

formation
of structures:

(droplet: nuclei)
rod
slab
tube
bubble

lower energy

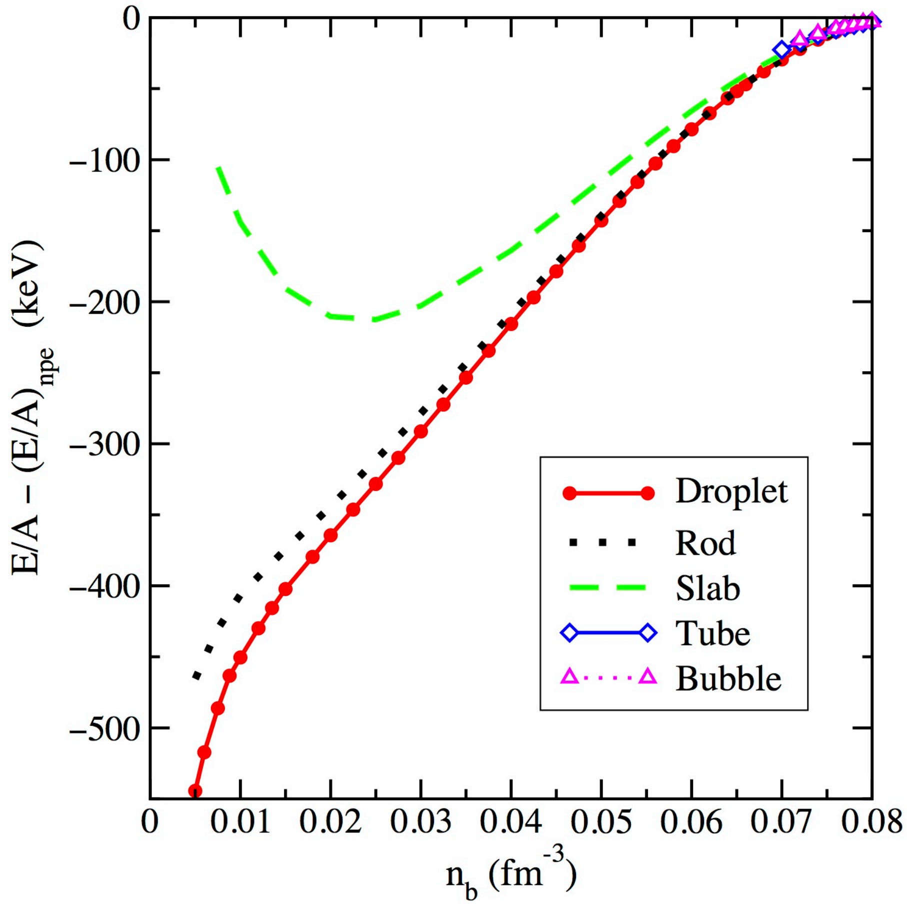

Fig. 3. Energy per baryon of different shapes relative to uniform *npe* matter as a function of baryon density in the inner crust.

B. K. Sharma et al., arxiv: 1506.00375

EOS at low densities from HIC

PRL 108, 172701 (2012) PHYSICAL REVIEW LETTERS week ending 27 APRIL 2012

Laboratory Tests of Low Density Astrophysical Nuclear Equations of State

L. Qin,[1] K. Hagel,[1] R. Wada,[2,1] J. B. Natowitz,[1] S. Shlomo,[1] A. Bonasera,[1,3] G. Röpke,[4] S. Typel,[5] Z. Chen,[6] M. Huang,[6] J. Wang,[6] H. Zheng,[1] S. Kowalski,[7] M. Barbui,[1] M. R. D. Rodrigues,[1] K. Schmidt,[1] D. Fabris,[8] M. Lunardon,[8] S. Moretto,[8] G. Nebbia,[8] S. Pesente,[8] V. Rizzi,[8] G. Viesti,[8] M. Cinausero,[9] G. Prete,[9] T. Keutgen,[10] Y. El Masri,[10] Z. Majka,[11] and Y. G. Ma[12]

Yields of clusters from HIC: p, n, d, t, h, α

chemical constants

$$K_c(A, Z) = \rho_{(A,Z)}/[(\rho_p)^Z(\rho_n)^N]$$

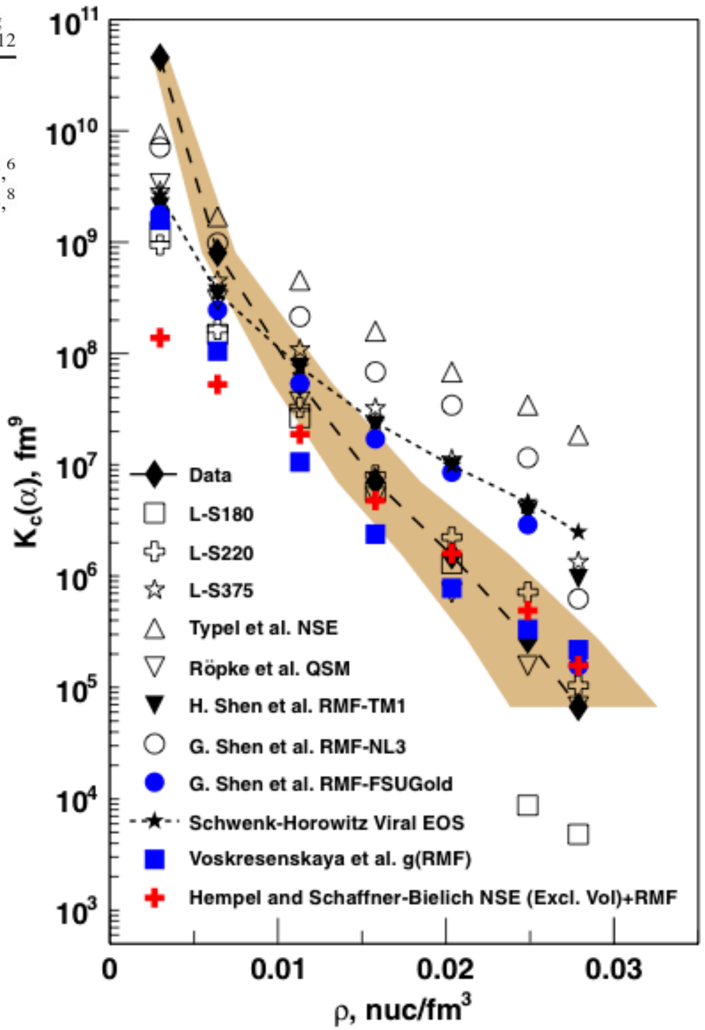

inhomogeneous,
non-equilibrium

Symmetry energy

Heavy-ion collisions, spectra of emitted clusters,
temperature (3 - 10 MeV), free energy

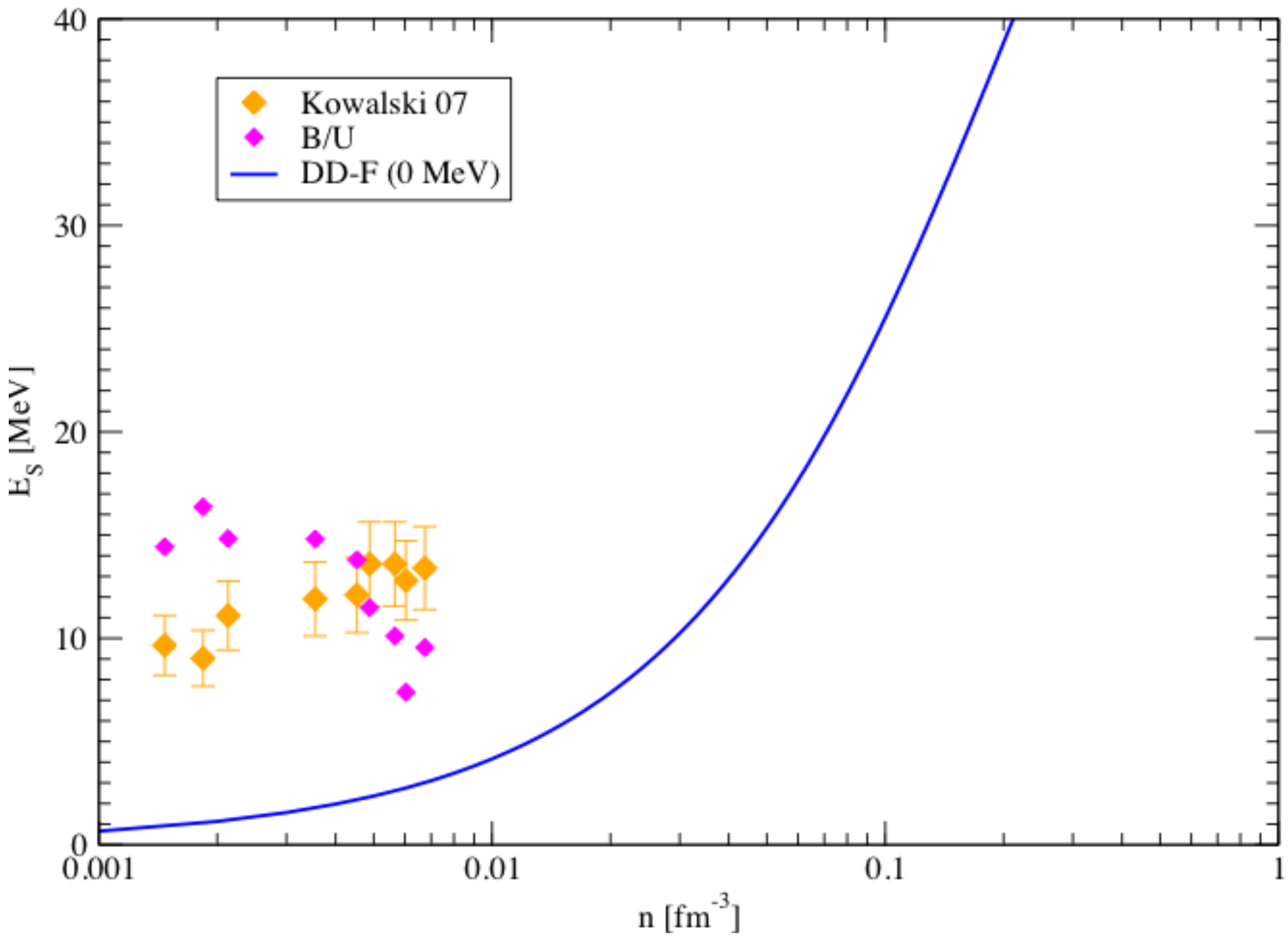

S. Kowalski et al.,
PRC **75**, 014601
(2007)

Symmetry energy: low density limit

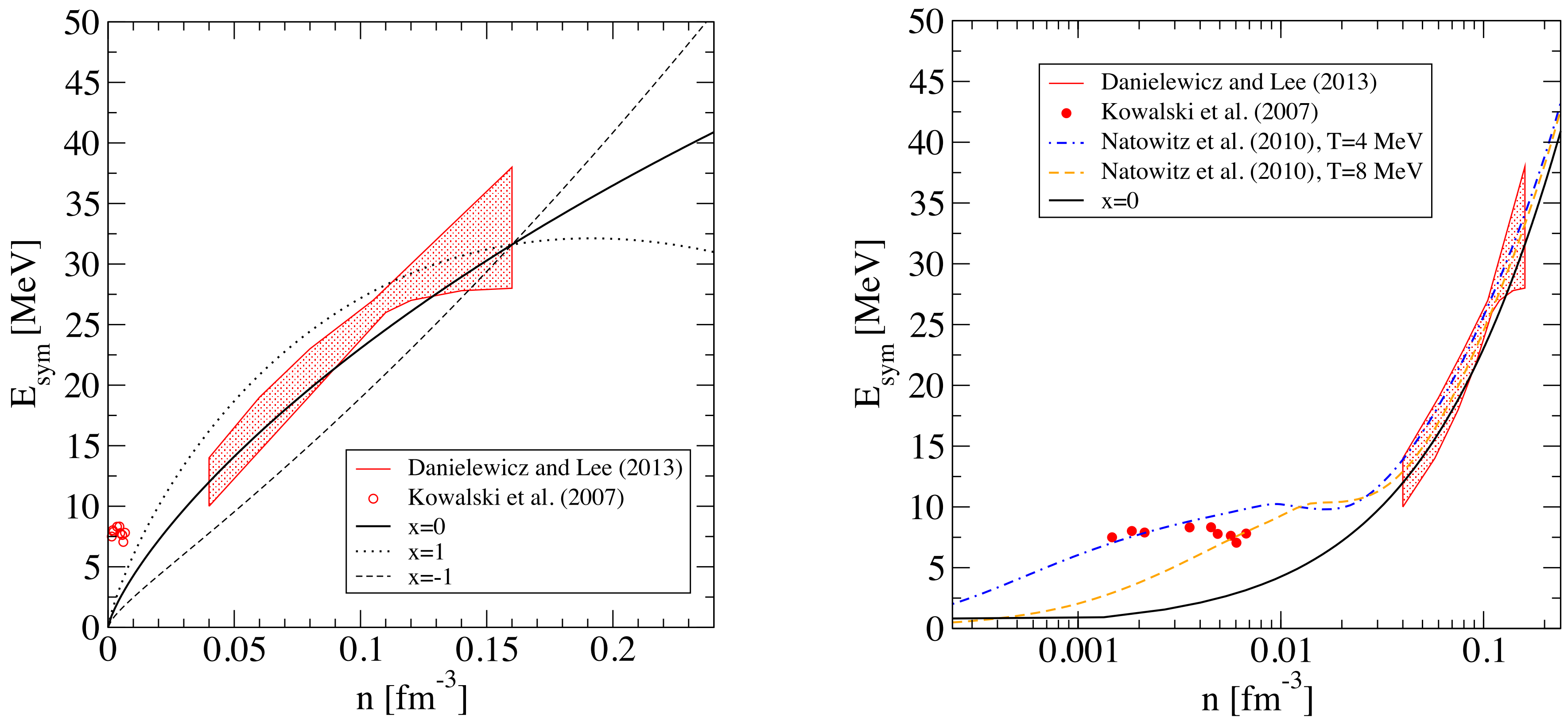

K. Hagel et al., Eur. Phys. J. A (2014) 50: 39

Formation of light clusters in heavy ion reactions, transport codes

PHYSICAL REVIEW C, VOLUME 63, 034605

Medium corrections in the formation of light charged particles in heavy ion reactions

C. Kuhrts,[1] M. Beyer,[1,*] P. Danielewicz,[2] and G. Röpke[1]
[1] *FB Physik, Universität Rostock, Universitätsplatz 3, D-18051 Rostock, Germany*
[2] *NSCL, Michigan State University, East Lansing, Michigan 48824*
(Received 13 September 2000; published 12 February 2001)

Wigner distribution

cluster mean-field potential

$$\partial_t f_X + \{\mathcal{U}_X, f_X\} = \mathcal{K}_X^{\text{gain}}\{f_N, f_d, f_t, \dots\}(1 \pm f_X) - \mathcal{K}_X^{\text{loss}}\{f_N, f_d, f_t, \dots\} f_X,$$

$$X = N, d, t, \dots .$$

loss rate

in-medium
breakup transition operator

$$\mathcal{K}_d^{\text{loss}}(P,t) = \int d^3k \int d^3k_1\, d^3k_2\, d^3k_3 |\langle k_1 k_2 k_3 | U_0 | kP \rangle|^2_{dN \to pnN} \times f_N(k_1,t) f_N(k_2,t) f_N(k_3,t) f_N(k,t) + \cdots . \qquad (3)$$

breakup cross section

$$\sigma_{\text{bu}}^0(E) = \frac{1}{|v_d - v_N|} \frac{1}{3!} \int d^3k_1\, d^3k_2\, d^3k_3 |\langle kP | U_0 | k_1 k_2 k_3 \rangle|^2 \times 2\pi\delta(E' - E)(2\pi)^3 \delta^{(3)}(k_1 + k_2 + k_3), \qquad (4)$$

Mott effect, in-medium cross section

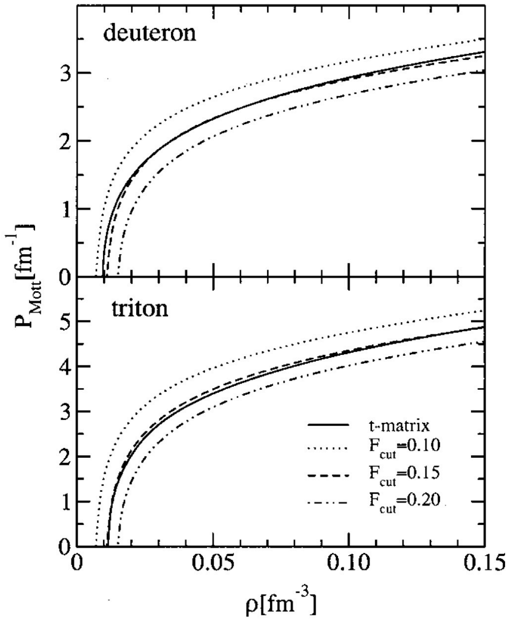

FIG. 1. Deuteron and triton Mott momenta P_{Mott} shown as a function of density ρ at fixed temperature of $T = 10$ MeV. The solid line represents results of the t matrix approach. The dashed, dotted, and dashed-dotted lines represent the deuteron Mott momenta from the parametrization given in Eq. (24) for three different cutoff values F_{cut}.

$$\int d^3 q \; f\left(\mathbf{q} + \frac{\mathbf{P}_{\mathrm{c.m.}}}{2}\right) \; |\phi(\mathbf{q})|^2 \leqslant F_{\mathrm{cut}}$$

C. Kuhrts, PRC **63**,034605 (2001)

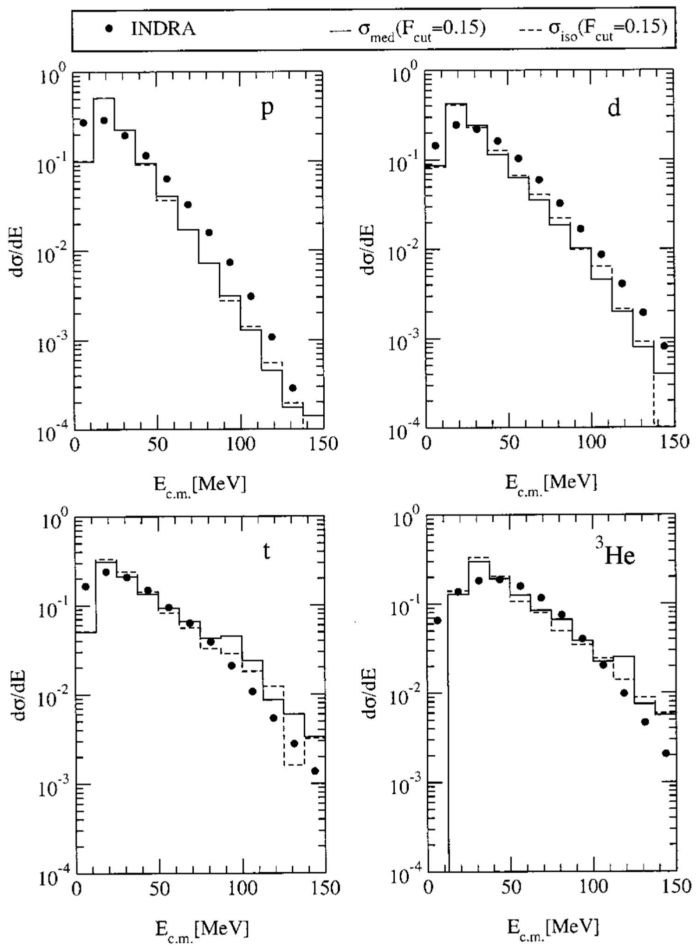

FIG. 5. Renormalized light charged light particle spectra in the center of mass system for the reaction ^{129}Xe+^{119}Sn at 50 MeV/nucleon. The filled circles represent the data of the INDRA Collaboration [21]. The solid line shows the calculations with the in-medium Nd reaction rates, while the dashed line shows a calculation using the isolated Nd breakup cross section; both with $F_{cut} = 0.15$.

Equilibrium correlations and transport codes

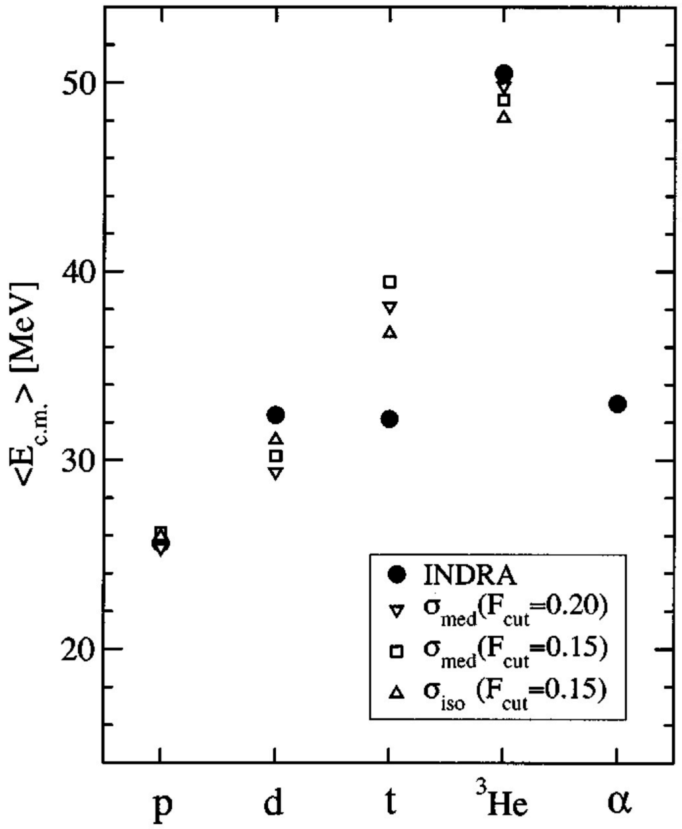

FIG. 6. Mean transverse energy of light charged fragments in the angular range of $-0.5 \leqslant \cos\theta_{c.m.} \leqslant 0.5$.

C. Kuhrts, PRC **63**,034605 (2001)

Important: Mott effect

Minor effects:
in medium cross sections

Missing: inclusion of alphas

Correlated continuum,
correlated medium

Freeze-out and local
thermodynamic equilibrium

single-particle quantum kinetic
equations and correlations

Equilibrium solution?

AMD (Akira Ono)

Summary

AMD has been extended to include cluster correlations.

- The correlation to bind several light clusters is also important.
- Transition from a wave packet to a plane wave is taken into account to improve nucleon spectra.

Clusters have strong impacts.

- Good reproduction of cluster and fragment productions, in various reaction systems simultaneously.
- The neutron/proton ratio is sensitive to the production of α particles (as well as to the density dependence of the symmetry energy).
- If clusters start to appear at early times, they change the way how the symmetry energy is reflected in final observables such as the π^-/π^+ ratio.

One-body dynamics ⇐ ⇒ Clusters

bulk properties (EOS)

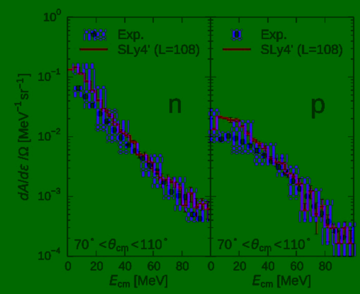

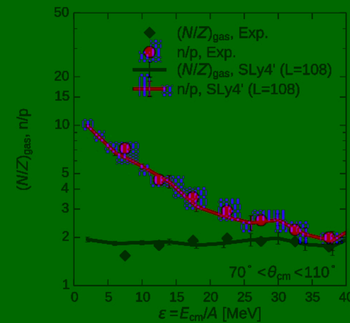

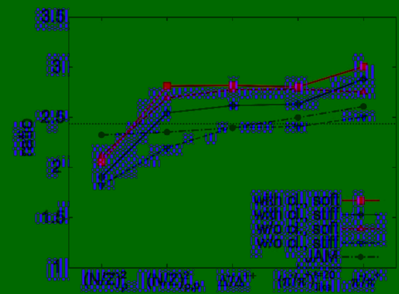

A cluster in medium & Clusterized nuclear matter

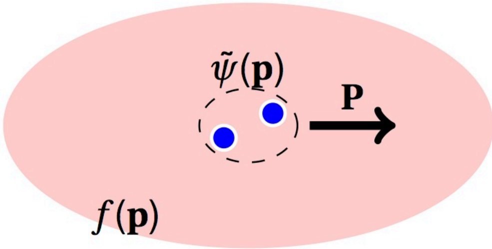

Equation for a deuteron in uncorrelated medium

$$\left[e(\tfrac{1}{2}\mathbf{P}+\mathbf{p})+e(\tfrac{1}{2}\mathbf{P}-\mathbf{p})\right]\tilde{\psi}(\mathbf{p})$$
$$+\left[1-f(\tfrac{1}{2}\mathbf{P}+\mathbf{p})-f(\tfrac{1}{2}\mathbf{P}-\mathbf{p})\right]\int\frac{d\mathbf{p}'}{(2\pi)^3}\langle\mathbf{p}|v|\mathbf{p}'\rangle\tilde{\psi}(\mathbf{p}')$$
$$=E\tilde{\psi}(\mathbf{p})$$

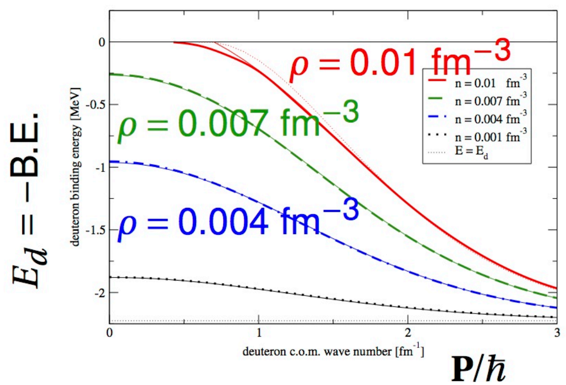

Momentum ($\mathbf{P}$) dependence of B.E.

Röpke, NPA867 (2011) 66.

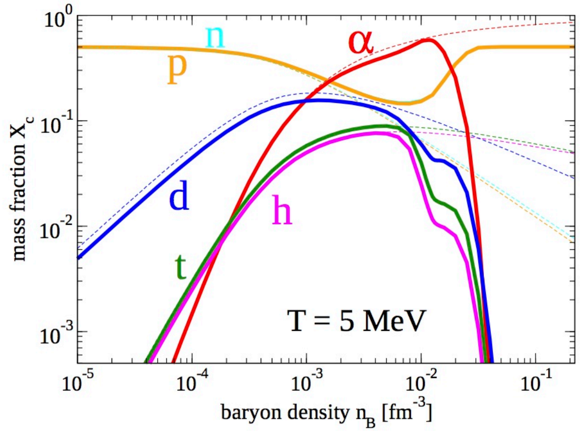

QS for symmetric nuclear matter

Röpke, PRC 92 (2015) 054001.

from A. Ono

Effect of cluster correlations: central Xe + Sn at 50 MeV/u

Without clusters

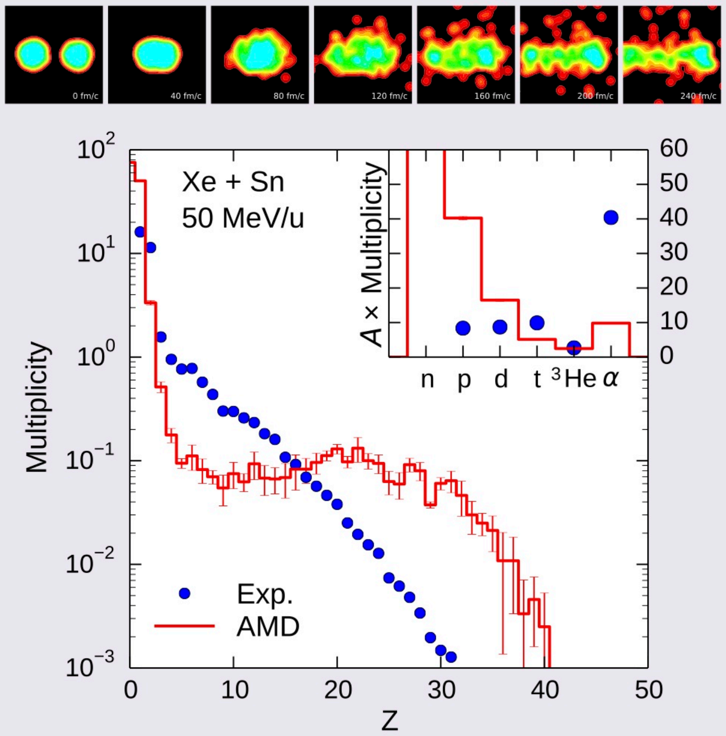

With clusters

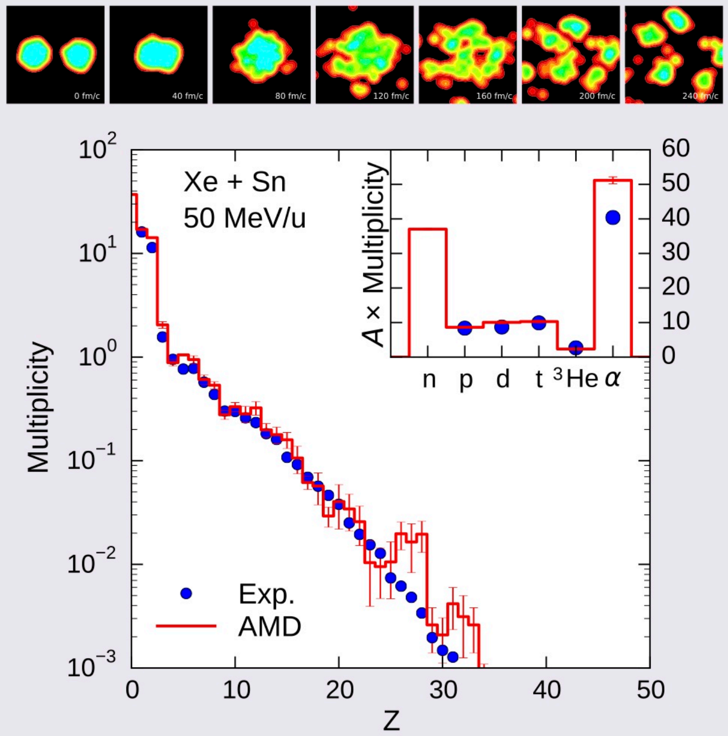

Light cluster production at NICA★

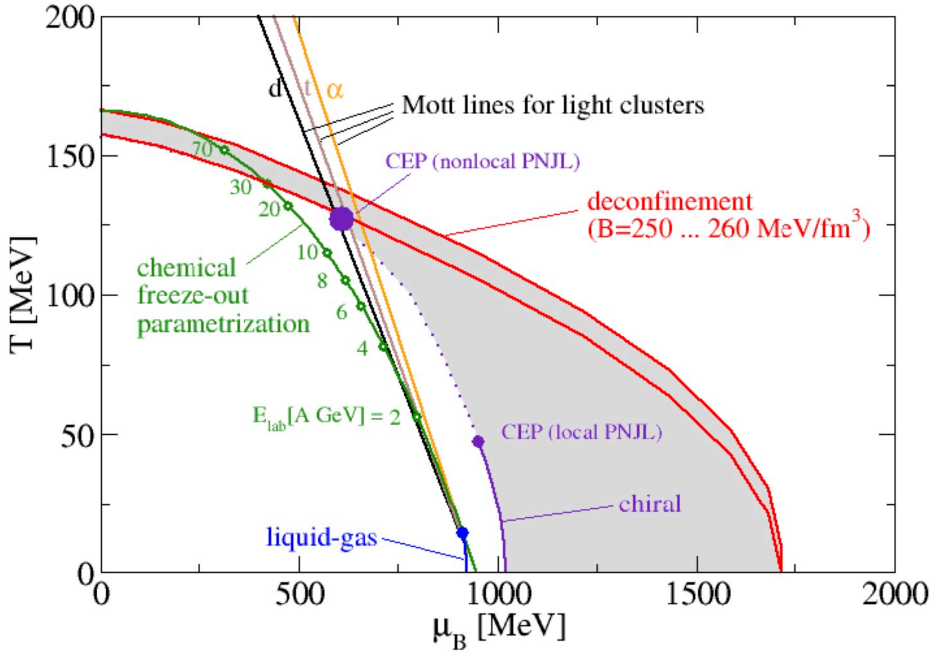

Fig. 1. Phase diagram of dense nuclear matter in the plane of temperature T and baryochemical potential μ_B. The diagram includes Mott lines for the dissociation of light nuclear clusters, extrapolated also to the deconfinement region. For details, see text.

N.-U. Bastian, P. Batyuk, D. Blaschke, P. Danielewicz, Yu.B. Ivanov, Iu. Karpenko, G. Ropke, O. Rogachevsky, and H.H. Wolter, Eur. Phys. J. A (2016) 52: 244

Light cluster production at NICA★

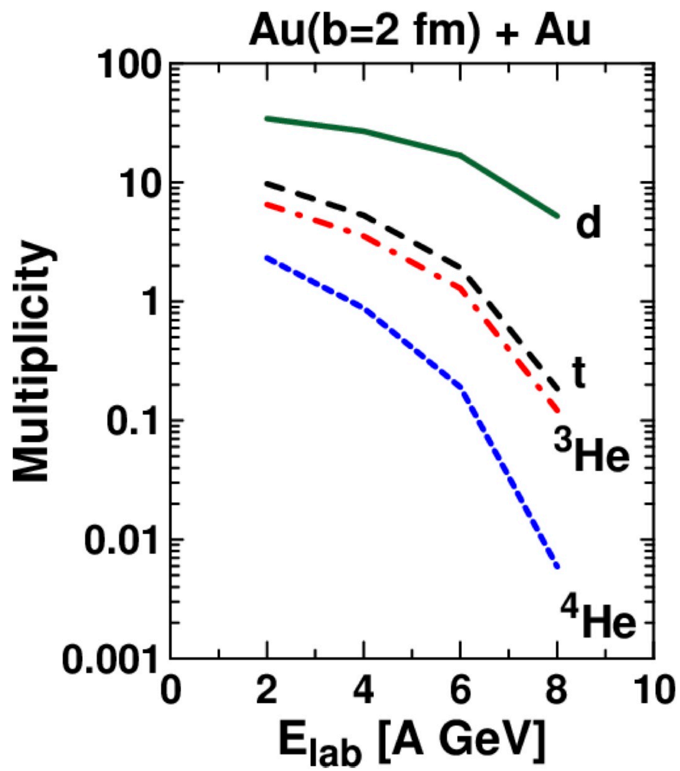

Fig. 5. Multiplicities of light clusters in central Au + Au collisions in the NICA energy range (calculated for an energy scan with $E_{\text{lab}} = 2, 4, 6, 8\,A\,\text{GeV}$). Results from a 3-fluid hydrodynamics description with cluster coalescence [22].

N.-U. Bastian, P. Batyuk, D. Blaschke, P. Danielewicz, Yu.B. Ivanov, Iu. Karpenko, G. Ropke, O. Rogachevsky, and H.H. Wolter, Eur. Phys. J. A (2016) 52: 244

Summary

• Quantum statistical approach: light clusters with in-medium quasiparticle energies. The Pauli blockiing is strongly depending on temperature T. Mott effect: bound states merge with the continuum

• The influence of continuum correlations (clusters) at increasing densities requires detailed investigations.

- Continuum correlations contribute to the symmetry energy (density dependent virial coefficients).
- The blocking of bound states is modified because of correlations in the medium (α matter).

• Dynamical response. Collective excitations, transport phenomena

• Relevant for HIC (freeze-out, transport theory) and astrophysics (supernova explosions: larger clusters (A>4), pasta structures)

Thanks

to D. Blaschke, C. Fuchs, Y. Funaki, H. Horiuchi,
J. Natowitz, T. Klaehn, Z. Ren, S. Shlomo, P. Schuck,
A. Sedrakian, K. Sumiyoshi, A. Tohsaki, S. Typel,
H. Wolter, Z. Xu, T. Yamada, B. Zhou
for collaboration

to you

for attention

D.G.

Light cluster production at NICA★

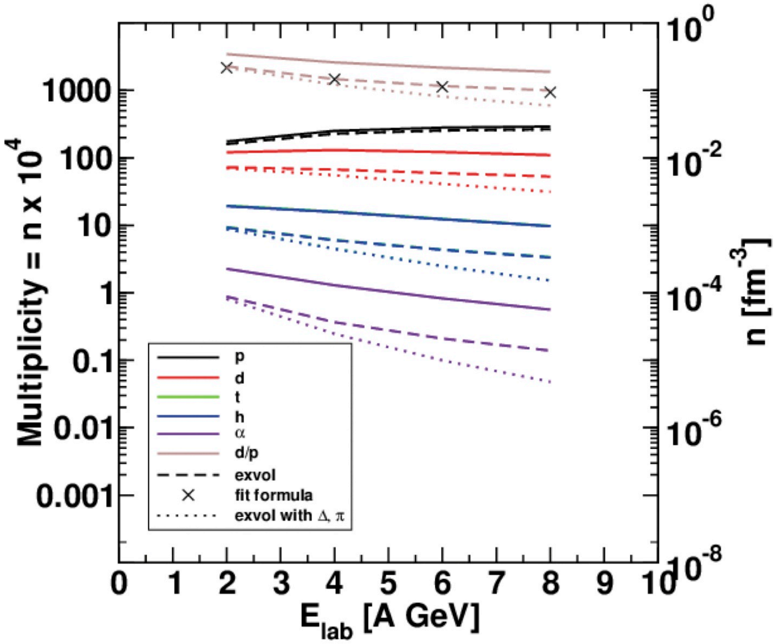

Fig. 2. Abundances of protons and of light clusters following LMA for temperature and chemical potential values along the freeze-out line eq. (1) in Au + Au collisions in the NICA energy range (anticipating an energy scan with $E_{\rm lab} = 2, 4, 6, 8\,A\,{\rm GeV}$). In each case solid lines are for the pointlike particles, dashed for the excluded-volume correction for nucleons and clusters, and dotted ones including also the volume of pions and deltas.

N.-U. Bastian, P. Batyuk, D. Blaschke, P. Danielewicz, Yu.B. Ivanov, Iu. Karpenko, G. Ropke, O. Rogachevsky, and H.H. Wolter, Eur. Phys. J. A (2016) 52: 244

EOS: continuum contributions

Partial density of channel A,c at P (for instance, $^3S_1$= d):

$$z_{A,c}^{\rm part}(\mathbf{P};T,\mu_n,\mu_p) = e^{(N\mu_n+Z\mu_p)/T}\left\{\sum_{\nu_c}^{\rm bound} g_{A,\nu_c}\, e^{-E_{A,\nu_c}(\mathbf{P})/T}\,\Theta\left[-E_{A,\nu_c}(\mathbf{P})+E_{A,c}^{\rm cont}(\mathbf{P})\right]+z_{A,c}^{\rm cont}(\mathbf{P})\right\}$$

separation: bound state part – continuum part ?

$$z_c^{\rm part}(\mathbf{P};T,n_B,Y_p) = e^{[N\mu_n+Z\mu_p-NE_n(\mathbf{P}/A;T,n_B,Y_p)-ZE_p(\mathbf{P}/A;T,n_B,Y_p)]/T}$$
$$\times g_c\left\{\left[e^{-E_c^{\rm intr}(\mathbf{P};T,n_B,Y_p)/T}-1\right]\Theta\left[-E_c^{\rm intr}(\mathbf{P};T,n_B,Y_p)\right]+v_c(\mathbf{P};T,n_B,Y_p)\right\}$$

parametrization (d – like):

$$v_c(\mathbf{P}=0;T,n_B,Y_p)\approx\left[1.24+\left(\frac{1}{v_{T_I=0}(T)}-1.24\right)e^{\gamma_c n_B/T}\right]^{-1}.$$

$$v_d^0(T)=v_{T_I=0}^0(T)\approx 0.30857+0.65327\;e^{-0.102424\;T/\mathrm{MeV}}$$

G. Roepke, PRC 92,054001 (2015)

Pauli blocking, correlated medium

In-medium Schroedinger equation

$$[E_{\tau_1}(\mathbf{p}_1;T,\mu_n,\mu_p)+\dots+E_{\tau_A}(\mathbf{p}_A;T,\mu_n,\mu_p)-E_{A\nu}(\mathbf{P};T,\mu_n,\mu_p)]\psi_{A\nu\mathbf{P}}(1\dots A)$$
$$+\sum_{1'\dots A'}\sum_{i<j}[1-n(i;T,\mu_n,\mu_p)-n(j;T,\mu_n,\mu_p)]V(ij,i'j')\prod_{k\neq i,j}\delta_{kk'}\psi_{A\nu\mathbf{P}}(1'\dots i'\dots j'\dots A')=0$$

effective occupation numbers

$$n(1)=f_{1,\tau_1}(1)+\sum_{B=2}^{\infty}\sum_{\bar\nu,\bar{\mathbf{P}}}\sum_{2\dots B}Bf_B\left(E_{B,\bar\nu}(\bar{\mathbf{P}};T,\mu_n,\mu_p)\right)|\psi_{B\bar\nu\bar{\mathbf{P}}}(1\dots B)|^2$$

effective Fermi distribution

$$n(1;T,\mu_n,\mu_p)\approx f_{1,\tau_1}(1;T_{\rm eff},\mu_n^{\rm eff},\mu_p^{\rm eff})$$

blocking by all nucleons

$$n(1;T,\mu_n,\mu_p)\approx\tilde f_{1,\tau_1}(1;T_{\rm eff},n_B,Y_p)$$

effective temperature $$T_{\rm eff}\approx 5.5\,{\rm MeV}+0.5\,T+60\,n_B\ {\rm MeV\ fm}^3$$

G. Roepke, PRC 92,054001 (2015)

Based on the one-body distribution function $f(\mathbf{r},\mathbf{p},t)$ $\Leftrightarrow$ One-body density matrix $\rho(\mathbf{r},\mathbf{r}')$

$$\frac{\partial f(\mathbf{r},\mathbf{p},t)}{\partial t} + \left\{f,\ h_{\text{MF}}[f]\right\} = I_{\text{coll}} + \text{fluct.}$$

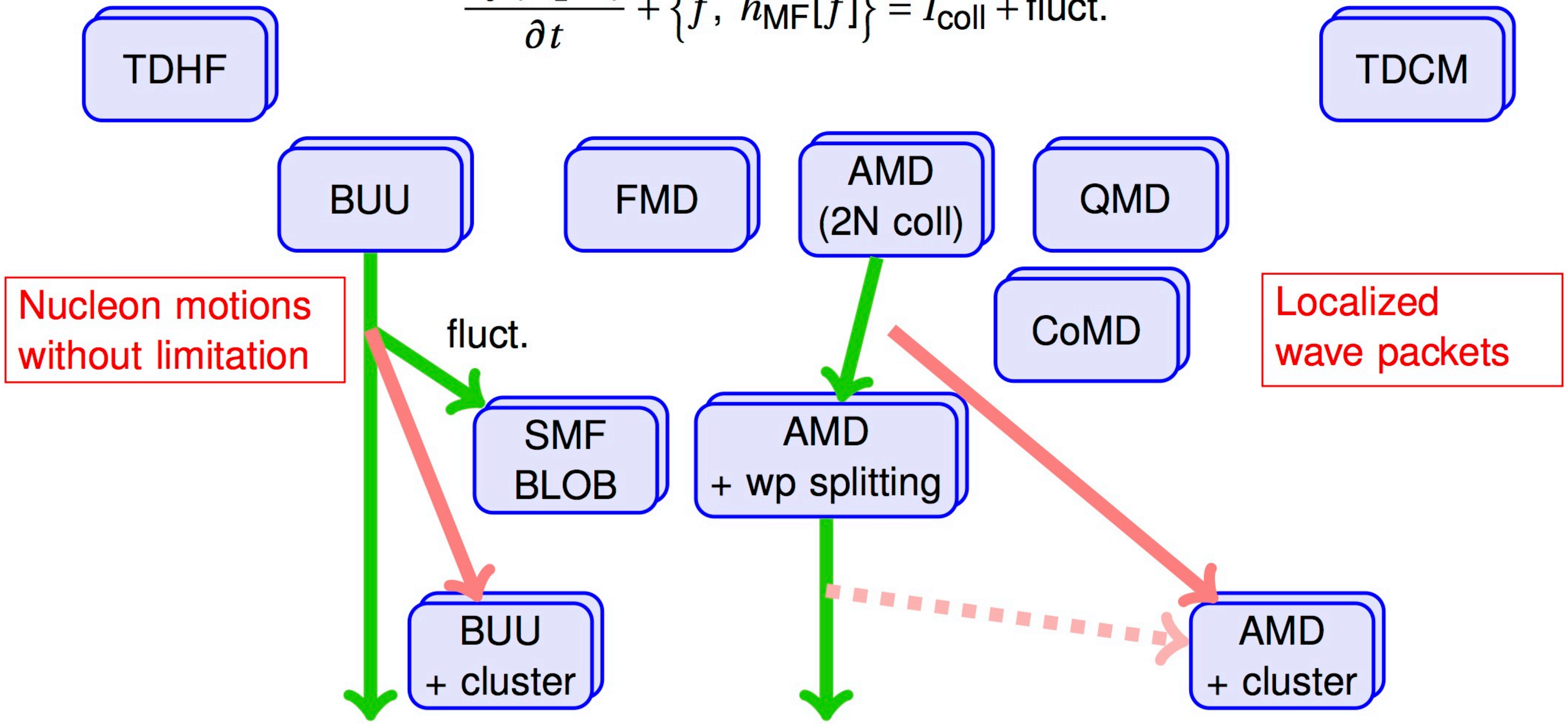

- Fluctuation/branching is a way to handle many-body correlations.
- Not many models treat cluster correlations explicitly.

Vaporized nuclei and nuclear matter

Heavy-Ion Collisions

Experimental data of cluster abundance in $^{36}Ar + ^{58}Ni$ for the events where the quasi-projectile is vaporized.

Borderie et al., EPJA6 (1999) 197, PLB388 (1996) 224.

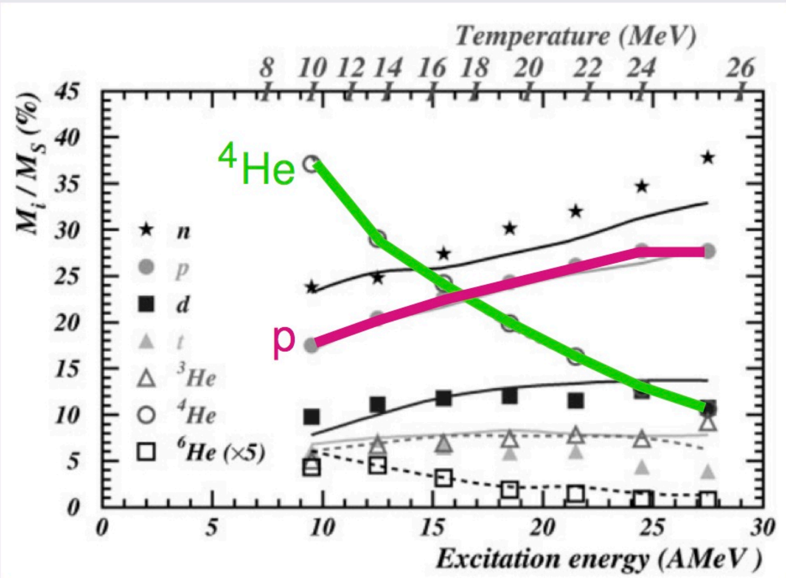

Supernova

Mass fraction of light clusters in the post-bounce supernova core, based on nuclear statistical equilibrium.

Sumiyoshi and Röpke, PRC77 (2008) 055804.

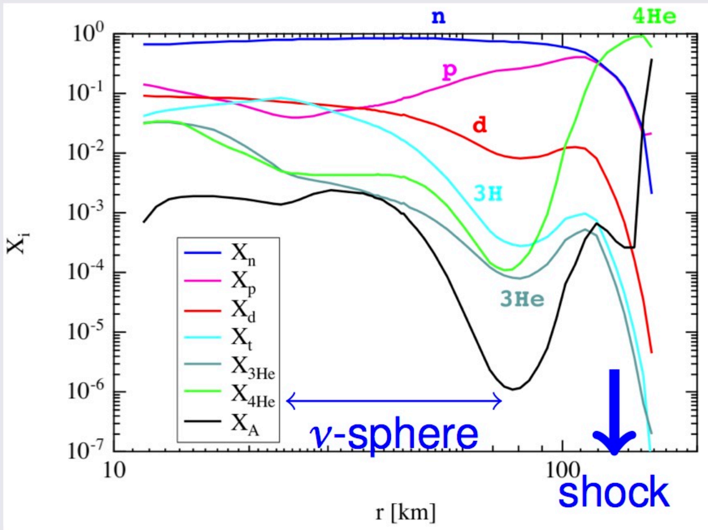

Neutron drip line

masses (binding energies) of neutron rich nuclei: ISOLDE experiment (CERN)

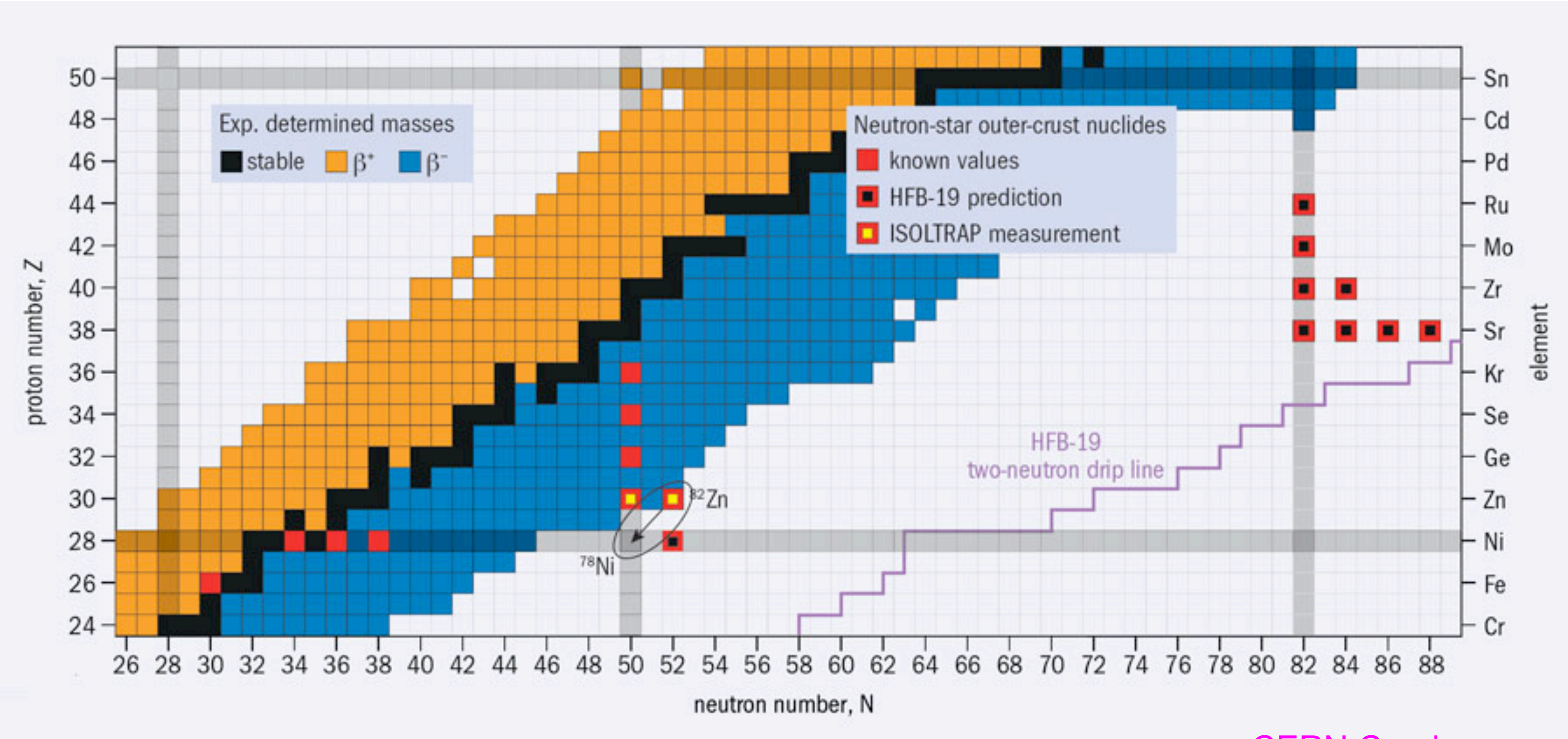

CERN Courier

experimental masses and mass models are input for the equation of state, the composition, and the structure of neutron stars

Various transport theories

Based on the one-body distribution function $f(\mathbf{r}, \mathbf{p}, t)$ $\Leftrightarrow$ One-body density matrix $\rho(\mathbf{r}, \mathbf{r}')$

$$\frac{\partial f(\mathbf{r}, \mathbf{p}, t)}{\partial t} + \left\{ f,\ h_{\mathrm{MF}}[f] \right\} = I_{\mathrm{coll}} + \text{fluct.}$$

Mean Field Models (BUU, VUU, BNV, SMF, BLOB, . . .)

"Nucleon motions in the mean field should be solved without any limitation."

Molecular Dynamics Models ($*$QMD, CoMD, AMD, . . .)

"Each nucleon should be localized because it has to be in a fragment at the end."

- Fluctuation/branching is a way to handle many-body correlations, even with the single-nucleon distribution function $f(\mathbf{r}, \mathbf{p}, t)$.
- Not many models treat cluster correlations explicitly.

Light cluster production at NICA★

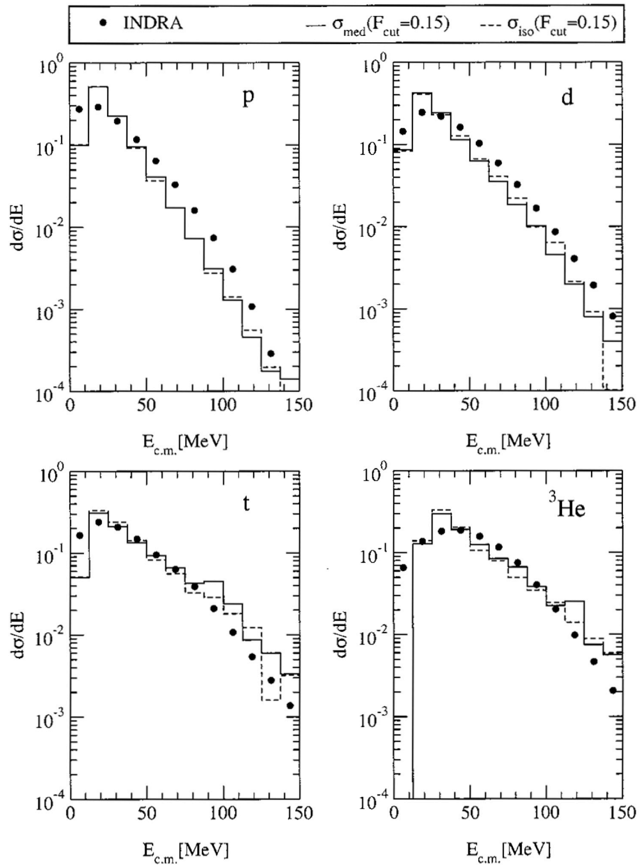

Fig. 3. Differential cross sections for production of charged $A \leq 3$ fragments in Xe + Se collisions at 50 MeV/nucleon. Results from the model of ref. [19] with cluster of mass $A \leq 3$ as explicit degrees of freedom.

N.-U. Bastian, P. Batyuk, D. Blaschke, P. Danielewicz, Yu.B. Ivanov, Iu. Karpenko, G. Ropke, O. Rogachevsky, and H.H. Wolter, Eur. Phys. J. A (2016) 52: 244

Boltzmann equation

- Relevant observables: single particle distribution function (classical, quantal)
- collisions
- Entropy
- Equilibrium solution
- Conservation of kinetic energy
- Time-dependent Green functions
- Spectral function
- quasiparticles

Transport codes, systems in non-equilibrium,
Mott effect and in-medium cross sections,
relevance of the equilibrium EoS.

Light cluster production at NICA★

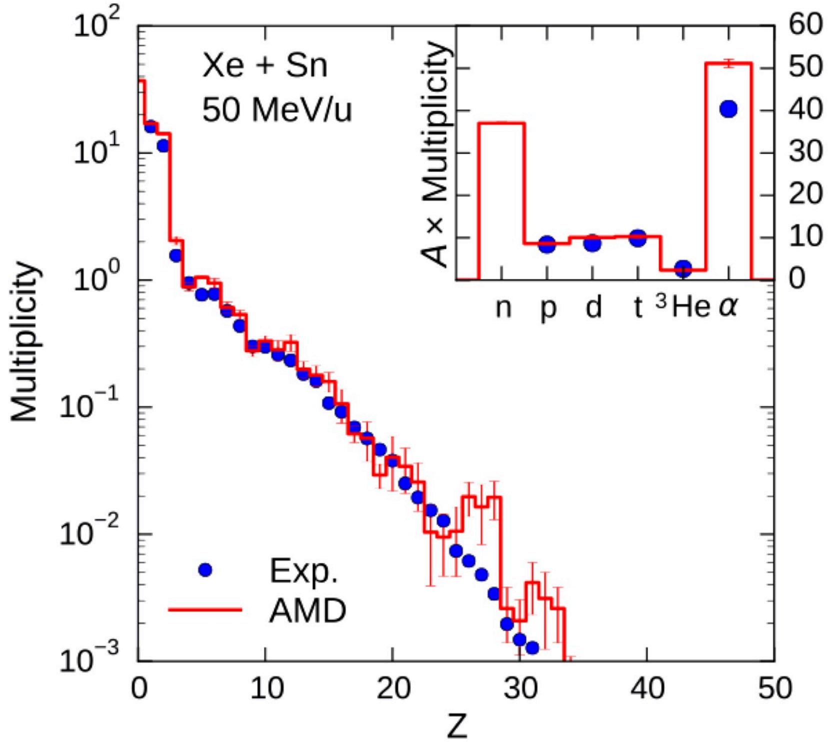

Fig. 4. Multiplicity of different charged fragments in Xe + Sn collisions at 50 MeV/nucleon. Results from the AMD model of ref. [20], including also heavier-cluster formation from cluster-cluster collisions.

N.-U. Bastian, P. Batyuk, D. Blaschke, P. Danielewicz, Yu.B. Ivanov, Iu. Karpenko, G. Ropke, O. Rogachevsky, and H.H. Wolter, Eur. Phys. J. A (2016) 52: 244

Light clusters and symmetry energy

dependent on T

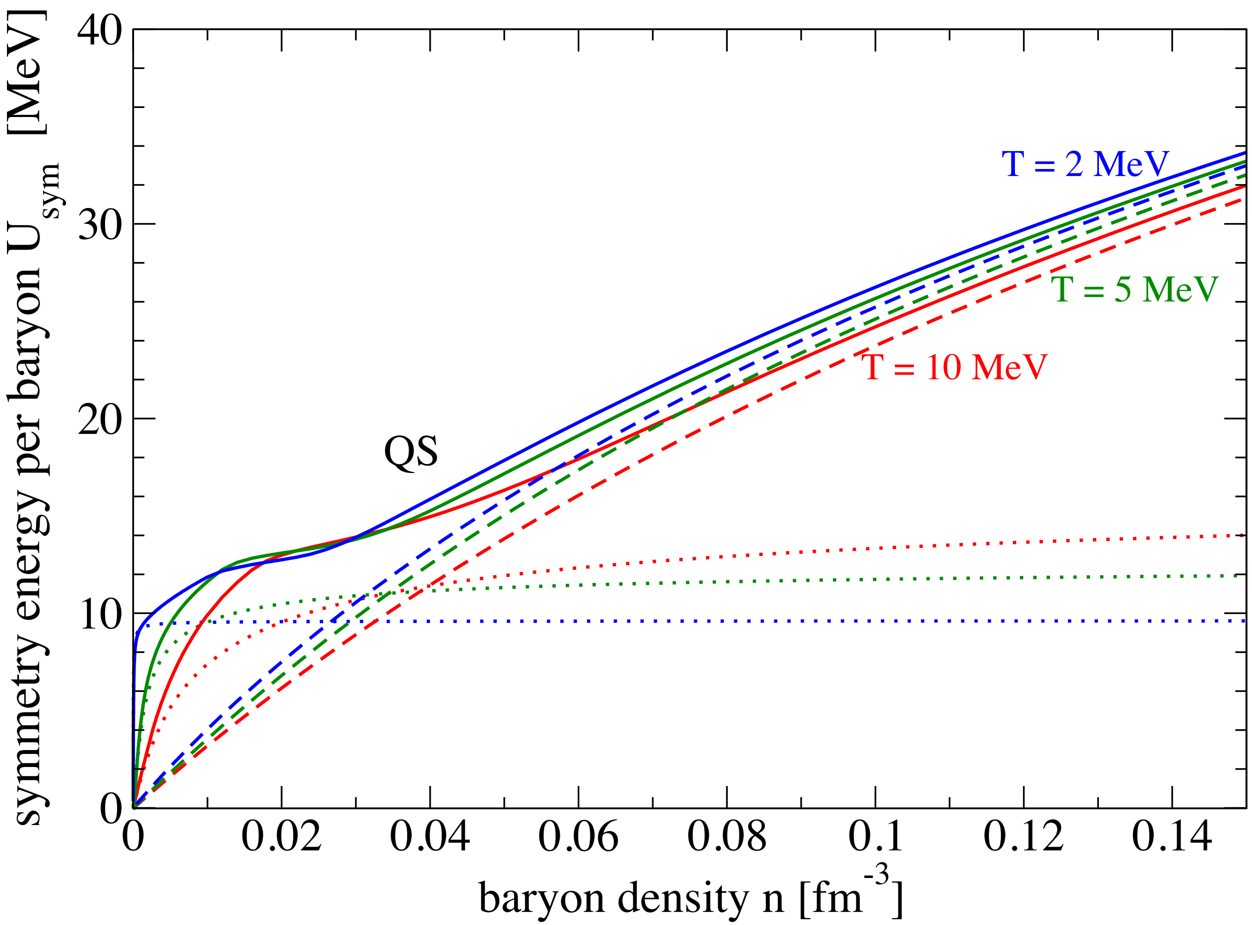

Full lines: QS
Dashed: RMF

Dotted: NSE

K. Hagel et al.Eur. Phys. J. A (2014) 50: 39

α cluster in astrophysics

Crust of neutron stars

Protons in droplets (heavy nuclei)

α−cluster outside, at the surface, condensate?

S. Typel, GSI

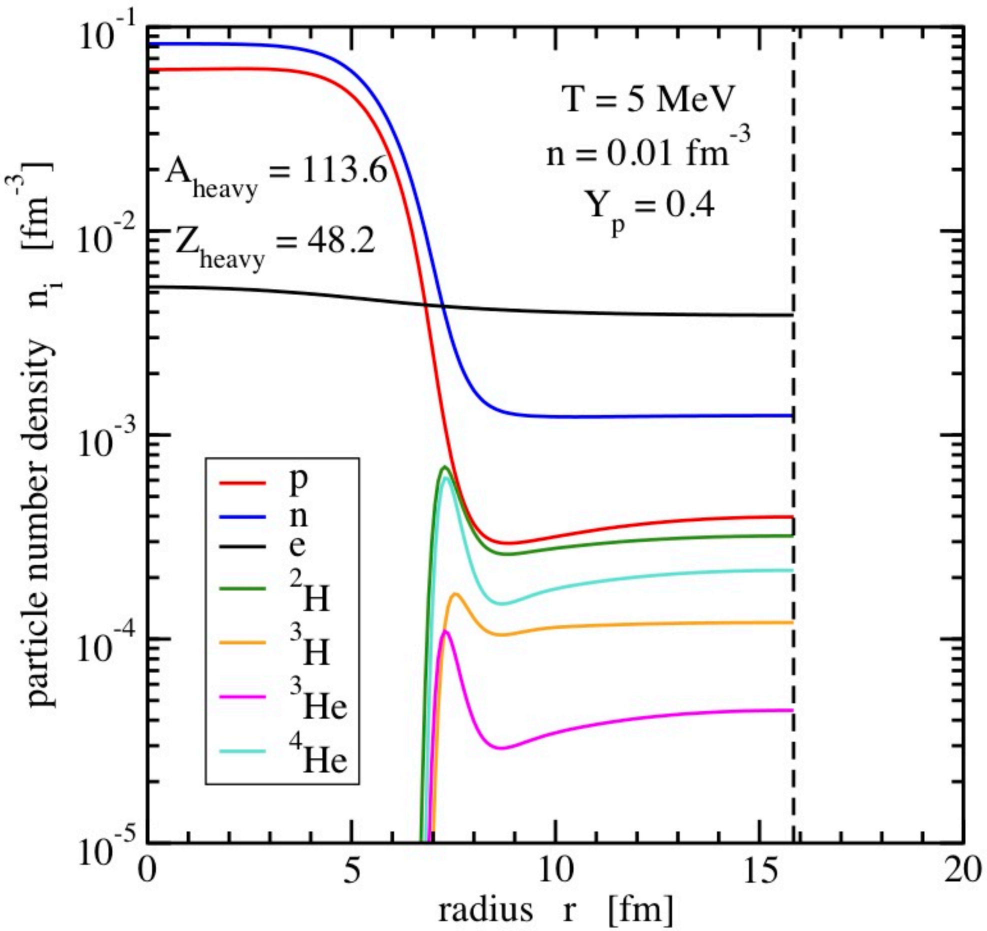

Core-collapse supernovae

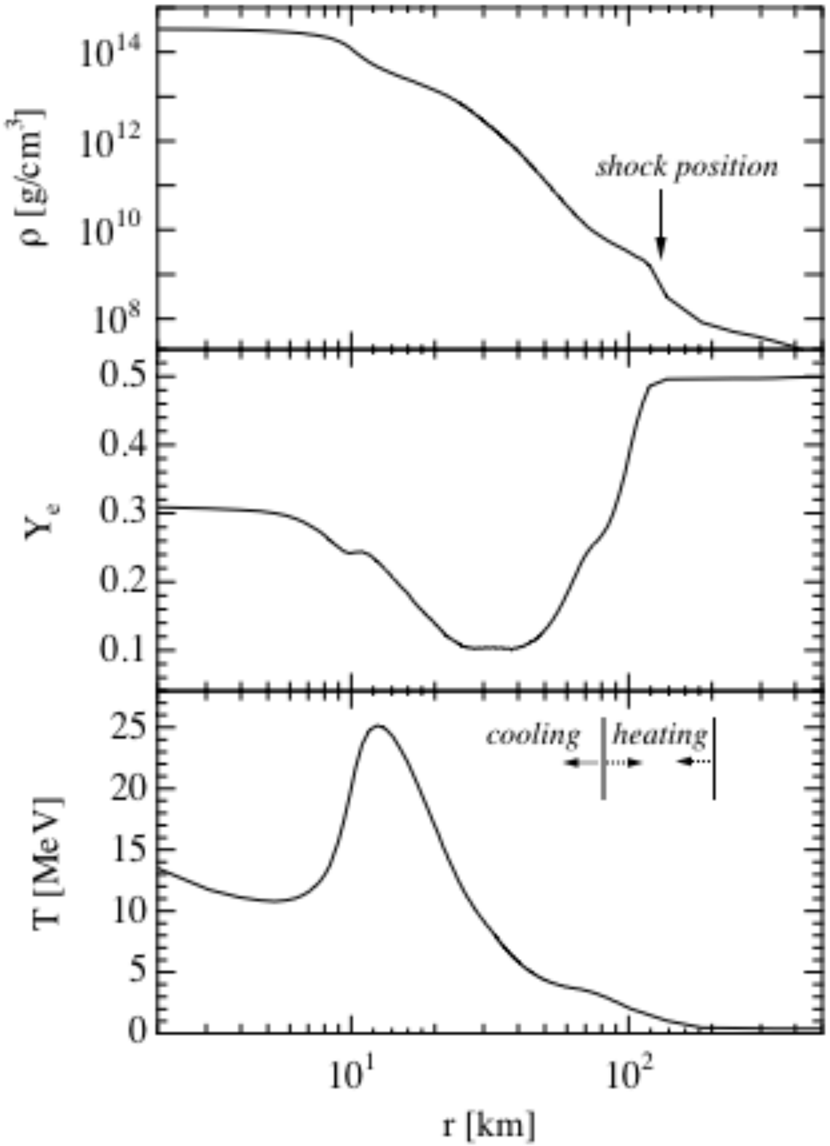

Density.

electron fraction, and

temperature profile

of a 15 solar mass supernova
at 150 ms after core bounce
as function of the radius.

Influence of cluster formation
on neutrino emission
in the cooling region and
on neutrino absorption
in the heating region ?

K.Sumiyoshi et al.,
Astrophys.J. **629**, 922 (2005)

Composition of supernova core

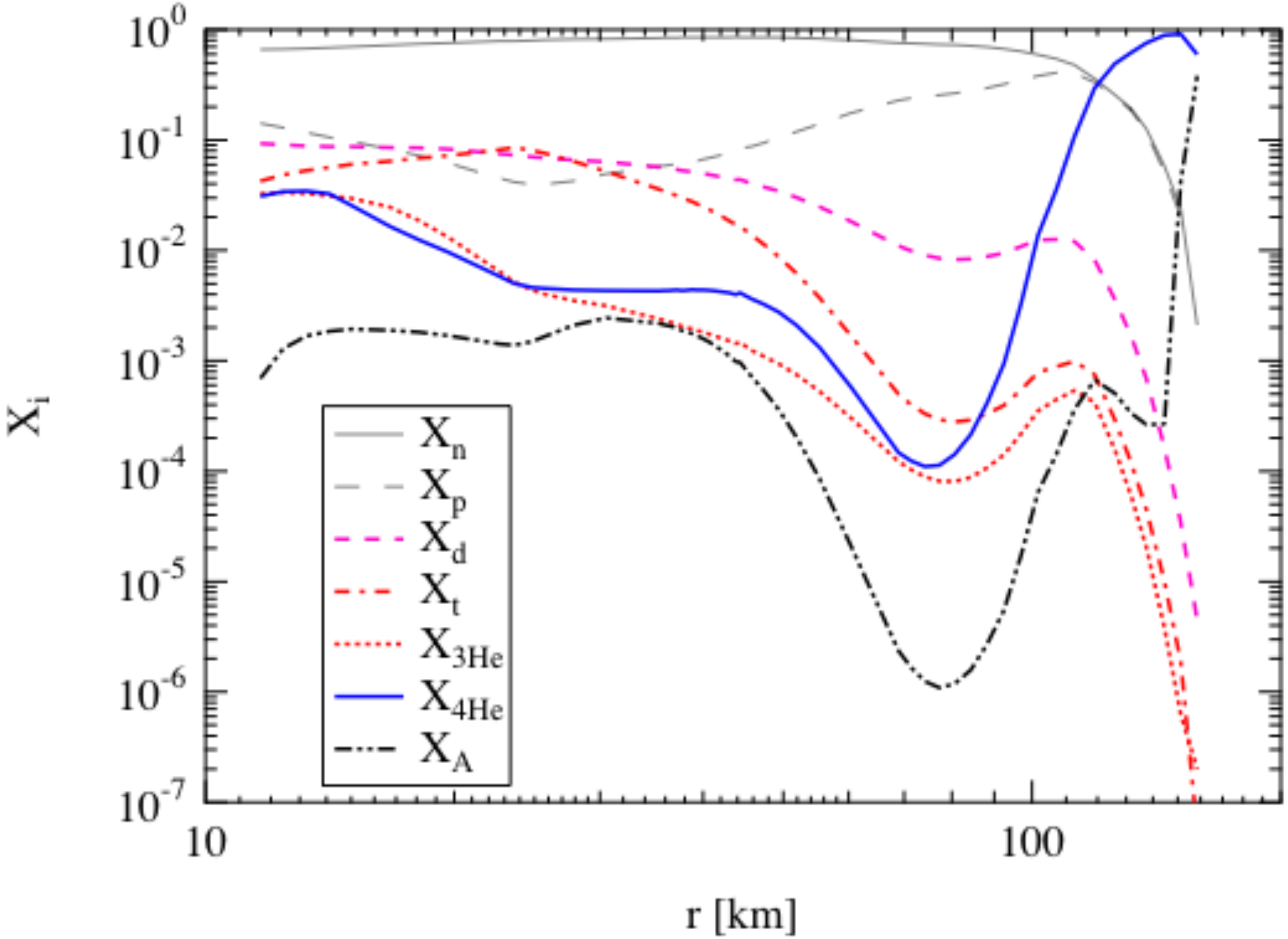

Mass fraction X of light clusters for a post-bounce supernova core

K.Sumiyoshi, G. R., PRC **77**, 055804 (2008)